Marine Pollution Bulletin 197 (2023) 115726

Contents lists available at ScienceDirect

Marine Pollution Bulletin

journal homepage: www.elsevier.com/locate/marpolbul

Quick and efficient microplastic isolation from fatty fish tissues by surfactant-enhanced alkaline digestion

Helge Torbjørn Bull Hove [a,1], Thomas Næsheim [a,b], Tanja Kögel [a,*]

[a] Institute of Marine Research, P.O. Box 1870 Nordnes, 5817 Bergen, Norway
[b] EUROFINS, Sandviksveien 110, 5035 Bergen, Norway

ARTICLE INFO

Keywords:
Microplastic
Extraction
Fish
Muscle
Recovery
μFTIR

ABSTRACT

For monitoring microplastic contamination in fish tissues, tissue digestion into filterable components prior to microplastic identification and quantification should be quick and efficient, providing satisfying microplastic recoveries of relevant particle sizes. Filtration with a small pore size, necessary to target small particles, is a challenge. Some proposed protocols take several days. To improve this, a combination of surfactants (Tween®-20 and Triton™ X-100) with potassium hydroxide (KOH) and pH neutralization was used. Fish bones were removed in tissue preparation prior to digestion. Recovery down to ca. 60–80 μm worked well for PA-66, PE, PET, PP, PS and PVC. In conclusion, we developed a comparatively swift digestion protocol, enabling filtration of 100 g samples with a pore size of 10 μm, for fish fillets with high (mackerel), intermediate (salmon, plaice) and low (cod) fat contents, fish liver, head kidney and oil samples, within 16–24 h.

1. Introduction

Plastic and rubber items, including car tires, fishing nets, ropes, synthetic paints, and packaging material erode by a multitude of mechanisms, shedding microplastics (MP). Additionally, MP are intentionally produced (Client_Earth, 2021). The impact of MP pollution on marine fish as well as on human seafood consumers is currently poorly understood. Toxic effects were identified for an array of wildlife species, based on laboratory exposure experiments showing MP particle bio-interference (Kögel et al., 2020), and effects by sorbed contaminants, such as POPS (Tang, 2021), personal care products (Atugoda, Vithanage et al., 2021), additives (Sridharan et al., 2022), and NIAS (non-intentionally added substances (Groh et al., 2019). As pointed out in these review articles, the relevance of modelled conditions to assess the risk for environment and human health are still far from satisfactory. Currently, the chemical methodology for the MP quantification has not reached the procedural maturity, efficiency, and standardization to support an extensive surveillance effort. Furthermore, quantification of small sized MP within a one and two-digit μm size range (and below) is required, but not yet feasible.

A significant challenge to the analytical quality assurance and quality control (QA/QC) routines is posed by the omnipresence of MP in the air (Munyaneza et al., 2022), and thereby on equipment and in chemicals (Primpke et al., 2022). Precautions such as filtered air, non-plastic shedding clothing worn by the lab personnel, and both negative and positive QC samples are required (Hermsen et al., 2018). For the quantification of small MP, end-point analysis by high-end instrumentation such as micro-Fourier Transform Infrared Microscopy (μFTIR) or Raman microscopy and pyrolysis-gas chromatography/mass spectrometry (py-GC–MS) or other applications of better quality should be used (Primpke et al., 2022) in preference to light microscopy, to ensure analytical selectivity.

Sampling and MP isolation remain the prime contributing factor to the measurement uncertainty for MP. This is even more pronounced when the study involves complex matrices such as fish (Kogel et al., 2022). Note also that the heterogenetic composition of different tissue types and organs poses a challenge to representative tissue sampling. Care should be taken in the creation of a proper and reproduceable sampling protocol. Although, on first sight, there seems to be an abundance of publications addressing the analysis of MP, measurement uncertainties (MU) in the analysis of small MP size classes, are not only high but often not even assessed. To arrive at a realistic measurement uncertainty description, it is pivotal to include the sampling and MP isolation procedures and not only the final analysis instrument variables.

* Corresponding author.
E-mail addresses: ThomasNaesheim@eurofins.no (T. Næsheim), tanja.kogel@hi.no (T. Kögel).
[1] Retired

https://doi.org/10.1016/j.marpolbul.2023.115726
Received 12 July 2023; Received in revised form 20 October 2023; Accepted 25 October 2023
Available online 3 November 2023

Without a reliable quantification of MP of all relevant sizes according to their chemical identity, in relevant matrices, there is no way to tell if effect studies reflect environmental conditions. Thus, the associated ecotoxicological risk cannot be assessed. This was illustrated by Isobe et al., 2019. Quantitative extraction protocols are urgently needed as an important link in the analytical chain of MP quantification. They should be time- and resource efficient to support monitoring programs with their large number of samples, as required to generate statistical power to study the fate and impact of MP. For fish, such knowledge is required for both food safety purposes as well as for oceanic stewardship for sustained ecosystem services.

The isolation of MP particles from fish matrices involves digestion of the tissue to the point where filtration of the sample is feasible using the analytically relevant pore size to retain the small MP that are the target analytes. Undigested matter, precipitation products or foams generated under the vacuum assisted filtration all counter the analytical goal of an acceptable filtration rate. A duration of hours, or a complete blockage of the filtration may occur if the matrix is digested insufficiently. Filter material, pore size, filtration apparatus, and digestion efficiency (DE%) were all found to be crucial factors impacting the filtration rate (Cole et al., 2014; Avio et al., 2015). The heterogenic chemical character of marine biological tissues affects their digestibility, challenging the prospect of a fit-for-all procedure. To degrade biological matrices, alkaline (e.g. KOH, NaOH), acidic (e.g. HNO_3, HCl, CH_3COOH) or oxidative chemicals (e.g. H_2O_2) have been used alone or in combinations (Welch et al., 2002; Vandermeersch et al., 2015; Wesch et al., 2016; Lusher et al., 2017; Miller et al., 2017; Lusher et al., 2020; Pfeiffer and Fischer, 2020; Bai et al., 2022). Acidic protocols reportedly solubilize the tissue well (Claessens et al., 2013; Karami et al., 2017; Naidoo et al., 2017), but excessive damage to sensitive polymers was reported (Van Cauwenberghe and Janssen, 2014; Catarino et al., 2017; Enders et al., 2017). Oxidative digestion protocols were less corrosive on polymers (Avio et al., 2015; Karami et al., 2017; Ding et al., 2018). However, they provide less effective matrix digestion with subsequent filtration issues due to foaming (Avio et al., 2015; Thiele et al., 2019). Protease, lipase and chitinase are commonly used enzymes (Loder et al., 2017; Primpke et al., 2018; Lusher et al., 2020). Enzymatic tissue digestion methods were promoted as gentle extraction protocols for MP particles (Cole et al., 2014; von Friesen et al., 2019) but require extensive time and often multiple procedural steps (Karlsson et al., 2017; Loder et al., 2017; Mintenig et al., 2017). Also, for this type of method, foam issues during filtration were reported (Thiele et al., 2019). Note that the high cost of these digestion agents is also a factor for consideration.

Alkaline protocols generally provided effective digestion while preserving the MP particles in terms of corrosive mass loss and/or visible surface damage of the investigated polymer types (Cole et al., 2014; Dehaut et al., 2016; Enders et al., 2017; Karami et al., 2017; Kuhn et al., 2017; Budimir et al., 2018; Ding et al., 2018; Phuong et al., 2018). Also surfactants provide a potential method to solubilize cellular material (Pata et al., 2004). Different surfactants can be considered due to their different properties. For example, Tween 20 is frequently used as a food emulsifier and ensures proper mixing of lipophilic and lipophobic components, while Triton-X-100 is frequently used in cell biological analysis to lyse cell membranes, such as in Kogel et al. (2013). An additional factor reported to negatively affect the MP analytical yield is the heat generated in or applied to the protocol, as heat may harm polymers (Karami et al., 2017; von Friesen et al., 2019).

Current published protocols are either specific to other target matrices than fish muscle or liver, or they are generalist protocols with unacceptable time and cost requirements, relying on expensive enzymes. Other published protocols are not suited or not tested for the preservation of target polymers for the vulnerable small sized MP particles (Thiele et al., 2021). Chemical vulnerability of MP is proportional to their relative surface area; thus, the smaller MP are more vulnerable than larger MP.

The Institute of Marine Research (IMR) identified a requirement for a new analytical method that encompassed these lessons, intended for the isolation of MP from selected seafood tissues and marine oils, for a high number of samples. The selection of tissues for the protocol intended to serve the purposes of seafood safety evaluation as well as ecotoxicological studies (Kögel et al., 2020). Fish are among others suggested as indicator species for environmental monitoring (Grosvik et al., 2022; Kogel et al., 2022). Very often, for analysis of MP in fish, only the gastrointestinal tract has been investigated. However, this provides a snapshot, reflecting diet MP load variations only, not what is taken up into vital organs, and often also not what is consumed by humans (Kogel et al., 2022). Furthermore, fish intestines are a problematic matrix reflected in poor DE% values for studies of small MP with resulting filtration issues, due to their extremely varied composition, reflecting the fishes diet. Since only small MP are taken up into fillet and liver (Gomiero et al., 2020), the study aim was to quantitatively isolate MP particles with size range down to 10 μm in its minor dimension of a 2D image when lying flat. Furthermore, the developed protocol should be capable of digesting larger and thus more representative samples of fish tissue than common in the current literature, to address seafood tissue heterogeneity issues: Since, with the current methods, numbers of particles >10 μm detected in fish fillet are on average below 1 per g (Gomiero et al., 2020), a larger amount of tissue is required in order to minimize random effects on the data. Contaminants in general are not dispersed homogeneously in the tissues and organs of fish, and smaller samples are more likely to misrepresent the MP contamination level. Expensive or time-consuming protocols (Foekema et al., 2013) are counterproductive for studies that require a high number of samples.

The aim of the study was to develop an analytical procedure, targeting fish fillets, fish liver and marine oils, with the capacity to handle a high number of samples to enable food safety monitoring. Sample amounts should be scaled to handle a sample size that addresses sample inhomogeneity issues. The procedure should encompass lessons from literature, and ensure a streamlined, quick, and robust protocol, as required for monitoring and surveillance purposes. The procedural conditions should – to the extent possible - not compromise polymer integrity, and the method should ensure acceptable recoveries of the relevant MP size range down to 10 μm.

The analytical method development was carried out in conjunction with and following up the project SalmoDetect (Gomiero et al., 2020). In the study at hand, several variants of a promising protocol were evaluated with the goal to evaluate and improve time, cost, efficiency, and polymer preservation. From the aim can be deduced that analysis time and laboratory resources, including man-hours, were to be prioritized. Thus, the number of steps should be minimized. Regarding the other relevant method descriptors: Several published protocols achieved acceptable or good scores for these, scores this study should be able to match, by implementing the lessons learned from them.

2. Materials and methods

2.1. Sampling and sample preparation

Haddock (*Melanogrammus aeglefinus*), European plaice (*Pleuronectes platessa*), Atlantic mackerel (*Scomber scombrus*), glacier lantern fish (*Benthosema glaciale*), and European hake (*Merluccius merluccius*) were collected from different surveys by the Institute of Marine Research (IMR), including surveillance projects by order of the ministry for Trade, Industry and Fisheries. Farmed Atlantic salmon (*Salmo salar*) was provided through the FHF (Fiskeri- og havbruksnæringens forskningsfinansiering) financed research project SalmoDetect (Gomiero et al., 2020). Marine oils from pelagic and mesopelagic species were provided from the ongoing research project MEESO at the IMR. Fat content of fish fillets are approximately 0.2 %, haddock; 1 %, plaice; 2 % hake; 3–30 % mackerel; 14–23 % salmon (https://seafood.no/globalassets/markedsforing/materiell/generelt/fakta-om-fisk.pdf). Fish liver contains higher percentages of fat, especially in lean fillet fish species

where fat is stored in the liver. Fish samples were prepared by cutting out the selected tissue, carefully avoiding fish scales and fish bones. Additionally, remaining fish bone fragments or scales were meticulously removed with the help of scalpel and tweezers. Fish tissue was thereafter cut into roughly 1 cm^3 large chunks with knives.

2.1.1. Contamination avoidance and monitoring

The entire process was carried out inside laminar flow benches in our MP clean laboratory with HEPA filtered air, sluice, sticky mat at the entrance, inside laminar flow benches, and with restricted access to the facilities. To monitor airborne MP contamination, open glass jars containing water were kept close to the real samples. A low number of contaminations were found: 0-few particles over 6–7 h, while each sample were exposed to the open air for only 5–10 min.

2.1.2. Chemicals, enzymes, and filters

The used chemicals are listed according to their suppliers: NaCl, KCl, Na_2HPO_4, KH_2PO_4, KOH, HCl (aq; 37 % m/m); Supelco® (Bellefonte, PA, USA); Tween®-20 (VWR International, Radnor, PA, USA); Triton™ X-100 (Millipore®, Burlington, MA, USA) and citric acid (Merck KGaA, Darmstadt, Germany). Ultrapure water was tapped from a Direct-Q® 3 UV Water Purification System (Millipore®). All prepared solutions were filtered through 0.7 μm glass fiber filters (VWR International) before use.

Concentrations of KOH (4.2 M), HCl (2.4 M) and citric acid (1 M) were the same in all experiments, however the ratios between matrix, KOH and saline surfactant solution were changed for optimization purposes during this study. Two different saline surfactant solutions were used: 1) PBS-surfactant ("PBSTnT")-solution: NaCl (1.4^{-1} M), KCl (2.7^{-3} M), Na_2HPO_4 (1.0^{-2} M), KH_2PO4 (1.4^{-3} M), Tween®20 ($1.7\bullet10^{-2}$ M) and Triton™ X-100 ($2.3\bullet10^{-2}$ M). 2) NaCl-surfactant ("NaTT")-solution: NaCl (1.5^{-1} M), Tween®20 ($2.4\bullet10^{-2}$ M) and Triton™ X100 ($3.4\bullet10^{-2}$ M).

Creon® pancrelipase (Mylan Healthcare, Canonsburg, PA, USA) contains a mixture of three enzymes: Lipase (25,000 Ph.Eur), amylase (18,000 Ph.Eur) and protease (1000 Ph.Eur). Creon® has previously been tested in MP protocols on bivalve tissue (von Friesen et al., 2019) and woodlice (Kallenbach et al., 2021). Protamex® is a Bacillus protease complex (Novozymes, Bagsværd, Denmark). The optimal temperature and starting pH for enzymatic hydrolysation of salmon using Protamex® has been determined to be 50–56 °C and pH 6.5–7.6 (Liaset et al., 2002).

Filtration 1: Digestates were first filtered on the following filters: Standard filter crucibles (10–16 μm (Por. 4), ROBU® Glasfilter-Geräte GmbH). For protocol 1c PTFE filter tiles (10 μm pore size, Bohlender GmbH), cut to 45 mm to fit equipment, cellulose nitrate (CN) filters (5 μm pore size, 47 mm diameter, Whatman®) and stainless-steel filters (10/500 μm pore size, Haver & Boecker, 47 mm diameter). All filters stayed flat in application, kept in place by the filter holder. The filter holder has an inner diameter of 3.6 mm. Due to the between-filter variability this text uses relative filtration time data if not indicated otherwise: The sample filtration time, divided by the filtration time of pure water, measured in the same filter. Filters with a time-deviation of >2× from the average filter were discarded.

Filtration 2: The filters used to isolate the MPs from the digested sample are unfit for subsequent analysis by μFTIR or py-GC–MS. The solid remains collected in the first filter had to be transferred to a second filter suited for that purpose. The following filters were tested for μFTIR: Anodisc (Whatman®, VWR, 0.2 μm pore size, 25 mm diameter), silver (Sterlitech, 5 μm sieve pore size, 25 mm diameter) and Teflon (Cole-Parmer, PTFE with PMP ring, 3 μm pore size, 25 mm diameter). These filters were also kept in place by the purpose-designed support ring, filter with ring available from producer, ensuring an optimal/flat operation. The filtration apparatus had an inner diameter of 1.5–1.6 mm.

2.1.3. HSE concerns

The corrosive and slippery nature of the alkaline solutions makes handling of these reagents as well as the sample solution a hazard, particularly during filtration, pH neutralization is of some help for this. As neutralization agent, HCl was replaced by the safer citric acid.

2.1.4. Digestion efficiency

The digestion efficiency (DE%) was calculated to measure the level of tissue solubilization as described by others before (Courtene-Jones et al., 2017; Karami et al., 2017; von Friesen et al., 2019; Bianchi et al., 2020).

$$DE\ (\%) = 100^{*}\left(1 - \left(\frac{F_{AP} - F_{BP}}{M}\right)\right)$$

The DE% was calculated from the mass difference of the crucible before and after protocol (F_{AP} and F_{BP} respectively) and the mass of the matrix (M). A high DE%, close to 100 %, indicates solubilization of most of the matrix. The goal of our study can be re-phrased in terms of DE%: A digestion of the selected seafood matrices to the point of feasible filtration through a 10 μm pore size filter, and to minimize matrix accumulation on the filter as required for a subsequent reliable identification of small MP by μFTIR. From experience, a DE% >99 % is required, and even higher DE% will be beneficial. However, the goal of achieving a high DE% may potentially have to be balanced against the study aim of also minimizing corrosive loss of MP mass and/or diameter, and thereby the risk of losing target MP through the filter pores.

2.1.5. Plastic polymer particles

Nurdles (approx. 3 mm) and smaller fragments (approx. 400–500 μm) of HDPE, LDPE, PA66, PC, PET, PMMA, PP and PS, along with 150 μm PVC spheres were received through our participation in the BASEMAN (JPI-OCEAN) project by partner UBAY (University of Bayreuth, Germany). Polymer group, product type, producer: PA-66, Ultramid, BASF; PC, Makrolon, Bayer Material Science; HDPE, Lupolen 4261 AG UV, LyondellBasell; LDPE, Lupolen 1800 P, LyondellBasell; PET, NEOPET 80, Neogroup; PMMA, PLEXIGLAS 7 N, Plexiglas; PP, HL508FB, Borealis; PS, Styrolution PS 158 N/L, INEOS Styrolution; PVC, Vinnolit S 3268, Vinnolit). The nurdles were delivered by producers to the BASEMAN project. To achieve smaller sized, irregular fragments for a realistic testing of MP recovery, the nurdles were cryo-milled at the IMR. Then, particles were sieved though an 80 μm sieve and further though a 63 μm sieve. What remained on the 63 μm sieve was characterized (Fig. S1) and used for recovery analysis. A size distribution analysis into several size ranges classified according to minimum diameter in μFTIR images in triplicates showed that the highest percentage of produced particles were within the range between 63 and 80 μm, but also particles below and above that range were present for PE, PP, PS and PVC, while PET MP size was slightly, and PA-66 and PMMA MP size distribution were heavily skewed towards the smaller sizes, while PC MP size distribution was skewed to the larger sizes (Fig. S1). 100 μm red PS spheres were acquired from Sigma-Aldrich (St. Louis, MO, USA). The smaller particles were stored in 70 % EtOH in a glass vial containing approximately 2 particles per μl. The mixture was shaken and immediately 50 μl were pipetted onto an Anodisc filter with the help of a syringe, and dried. The number, polymer type and size of particles were then analyzed by μFTIR. The Anodisc filter was then dissolved by immersing it in KOH:NaTT (1 part:2 parts; see paragraph "Chemicals and Enzymes") over night as for protocols 1b/c. The solution containing the MP was then filtered again and analyzed by μFTIR (Fig. S1). After treatment PC, PE, PET and PP size distribution had slightly shifted towards smaller size, while PS and PVC maintained their size distribution approximately as before. PA-66 shifted distribution towards larger size; agglomeration cannot be excluded (Fig. S1). For recovery testing with matrix, red PS beads of 100 μm (Sigma-Aldrich) were added into a glass petri-dish and counted (92–121 MP) and washed into the matrix, which thereafter was digested with

protocol 1b.

2.1.6. Equipment and particle identification

All filtration was carried out with vacuum assistance, using a diaphragm pump (Gardner Denver Thomas GmbH Welch Vacuum, Fürstenfeldbruck, Germany). Filters with the collected solid matter deposits, were examined using a handheld digital microscope (20-220x, 1.3 MP Resolution) equipped with white LED/UV excitation LED (EX: 400 nm, EM 430 nm; AnMo Electronic Corp. Hsinchu, Taiwan) DinoLight. 5-digit anti-static scale (METTLER TOLEDO, XSR225 DualRange, Switzerland), high temperature laboratory oven LHT 6/60 (Carbolite Gero, Sheffield, UK), Nicolet™ Summit PRO FTIR spectrometer equipped with the Everest™ ATR accessory monolithic ATR crystal (ThermoFisher Scientific™, Waltham, MA, USA), to collect the spectra from 4000 cm^{-1} to 400 cm^{-1}. For each sample 16 co-added scans with spectral resolution of 4 cm^{-1} were collected and 16 pre-recorded background scans were used for correction. Spectra were processed in the OMNIC Paradigm Desktop software (Thermo Scientific™) and compared to spectra of known compounds and polymers in commercial libraries (Thermo Scientific™) and in-house libraries. μFTIR imaging was performed using an Agilent Cary 620 FTIR microscope coupled to a Cary 670 FTIR spectrometer with a liquid nitrogen cooled 128 × 128 Focal Plane Array (FPA) detector, allowing for imaging of 128 × 128 pixels in a single measurement, a MIR Source with a spectral range of 9000–20/cm, purged enclosure, 15x IR/Vis reflective objective (NA 0.62, WD: 21mm), 4x Vis glass objective (NA 0.2, WD: 38 mm), motorized sample stage, 0.1 × 0.1 MCT (Agilent, Santa Clara CA, USA). Each pixel was imaged for the whole spectrometric range. For dataset analysis, data was processed by siMPLE (v.1.0.0; simple-plastics.eu) and spectra were compared to libraries from Bio-Rad and Agilent, the Alfred-Wegener Institute Helgoland (Primpke et al., 2018) and IMR with the help of simple and MPHunter (https://simple-plastics.eu/about.html; combined interface freeware). Simultaneous optical images are used to obtain the size of the particles in two dimensions. Automatic image processing assigns a polymer group to the particles. Py-GC–MS was performed with a Frontier Lab Multi-Shot Pyrolyzer™ (EGA/PY-3030D) with Auto-Shot Sampler™ (AS-1020E; Frontier Lab, Koriyama, Japan), coupled to a Thermo Scientific™ TRACE™ 1310 Gas Chromatograph with a Thermo Scientific™ TraceGOLD™ TG-5SilMS 30 m × 0.25 mm I. D. ×0.25 μm film capillary column (P/N 26096-1420; ThermoFisher Scientific™, Waltham, MA, USA), coupled to a Thermo Scientific™ Exactive™ GC Orbitrap™ mass spectrometer, as described in Toto et al. (2023).

2.1.7. Systematic literature search

The search-string (Microplastic*) AND (extraction* OR digestion* OR method*) AND (fish* OR tissue* OR biota OR meat* OR flesh OR muscle*) was used for a literature search to compare methods used for digesting fish muscle tissue to our study (Table 3: Literature comparison of studies investigating methods for digesting fish muscle tissue3). Chemicals, DE%, time and cost, filters, filtration, and polymer recovery according to size were extracted and compared.

2.1.8. Statistical methods

Calculations and statistical analyses were performed with Excel (Office, Microsoft) or Statistica™ 13 (StatSoft Europe, Hamburg). Difference between groups was tested with the nonparametric Kruskal-Wallis test. Results are deemed significant when $p < 0.1$. If not declared otherwise, errors are provided as standard deviation.

3. Results and discussion

Dehaut et al. (2016), Karami et al. (2017), Süssmann et al. (2021) and the current study evaluated previous studies on performance criteria such as time requirement, digestion rates and polymer integrity and then developed their own protocol for fish fillet digestion further, based on KOH. In the current study, improvements to filtration rates, with a major determinant of that being the DE%, were chosen as the primary means by which the protocol was to reach a reduction in man-hours, occupation of lab-resources and required protocol steps. The experiments confirmed that the primary bottleneck was the filtration with its associated issues of clogging and foaming. Thus, filtration rate was selected for the prioritized metric to evaluate protocols, granted that the optimized protocol could be documented to preserve polymer integrity sufficiently to provides acceptable recoveries of MP of the targeted size range and polymer types.

3.1. Preliminary improvements of digestion protocol

The first matrix tested for the experiments was salmon fillet, a species of high commercial value, production volume and with an intermediate fat content among fish species. The first protocol was an established alkaline (KOH) protocol at 40 °C (Karami et al., 2017), avoiding higher temperatures that could potentially damage the MP (Dehaut et al., 2016; Munno et al., 2018; Thiele et al., 2019) and lower temperatures, avoiding low DE% (von Friesen et al., 2019; Süssmann et al., 2021) (Protocol 1a, see below). This initial protocol spawned a series of potentially improved versions. Each of them was assessed through procedural descriptors like analysis time, DE%, and MP vulnerability, based on a series of experiments. Generally, the analytical aim for a smaller MP size is counteracted by incomplete digestion products clogging the fine pores in the filter. Thus, filtration-time became the limitation to feasible pore sizes for a successful analysis (Cole et al., 2014). Thiele et al. (2019) found that KOH digestion of mussels without a neutralization step, allowed filtration <25 μm, while further optimization by pH neutralization using citric acid, facilitated filtration down to 1.2 μm. Thiele et al. (2019) also compared protocols and found the highest individual MP recovery in a KOH based protocol at 91.6 %, with a mean recovery of 78 %. Sample shaking during digestion may partly aid DE% (Süssmann et al., 2021). In the current study, samples were frozen prior to the digestion protocol which may have aided the digestion, as the freezing-thawing process may break cell membranes (Bodzon-Kulakowska et al., 2007).

Initially, the following protocols were compared (Fig. 1):

Protocol 1a (KOH-"PBSTnT"): A protocol was designed at IMR for participation in the interlaboratory test exercise of BASEMAN (JPI-OCEANS), where the study aim was to compare digestion protocols for farmed salmon intestines, haddock intestines and blue mussels. The protocol has not been published before: 100 g sample tissue was transferred to an 1 l Erlenmeyer flask. 200 g "PBSTnT" solution was used to aid the transfer and to dilute the sample to disperse the sample and to damage cell membranes with the detergents. The solution was buffered, as it was used for direct comparison of the performance with enzymatic digestion, and to provide a stable environment and to avoid denaturation of proteins, which may potentially slow down degradation. In short, the samples of 100 g each were placed in an orbital shaking incubator at 56 °C at 130 rpm for 16 h in 200 g PBSTnT. 200 g of 4.2 M KOH solution was slowly added to each Erlenmeyer flask. Resulting in 2.4 M KOH, and the flasks were again shaken for 3 h at 56 °C and 130 rpm. 400 g water was added to each sample, and the samples were left to settle for 1 h at 56 °C before filtration. Observations from the BASEMAN (JPI-OCEAN) experiments, suggested an incomplete digestion after 3 h. Thus, the procedure was modified as follows:

For the current study the 4.2 M KOH solution was added early, together with PBSTnT, to 2.4 M, the temperature was adjusted to 40 °C, based on the work of Karami et al. (2017), while keeping the incubation time at 24 h.

Protocol 1b (KOH_"NaTT"-1): This protocol was developed for the SalmoDetect project (Gomiero et al., 2020). The protocol, applied to 400–500 μm particles (as used in this study) and 150 μm PVC particles, without matrix, gave recoveries from 72 to 95 % (PVC) to 90–102 % (PE) with the exception of 68–80 % for polymethyl methacrylate (PMMA)

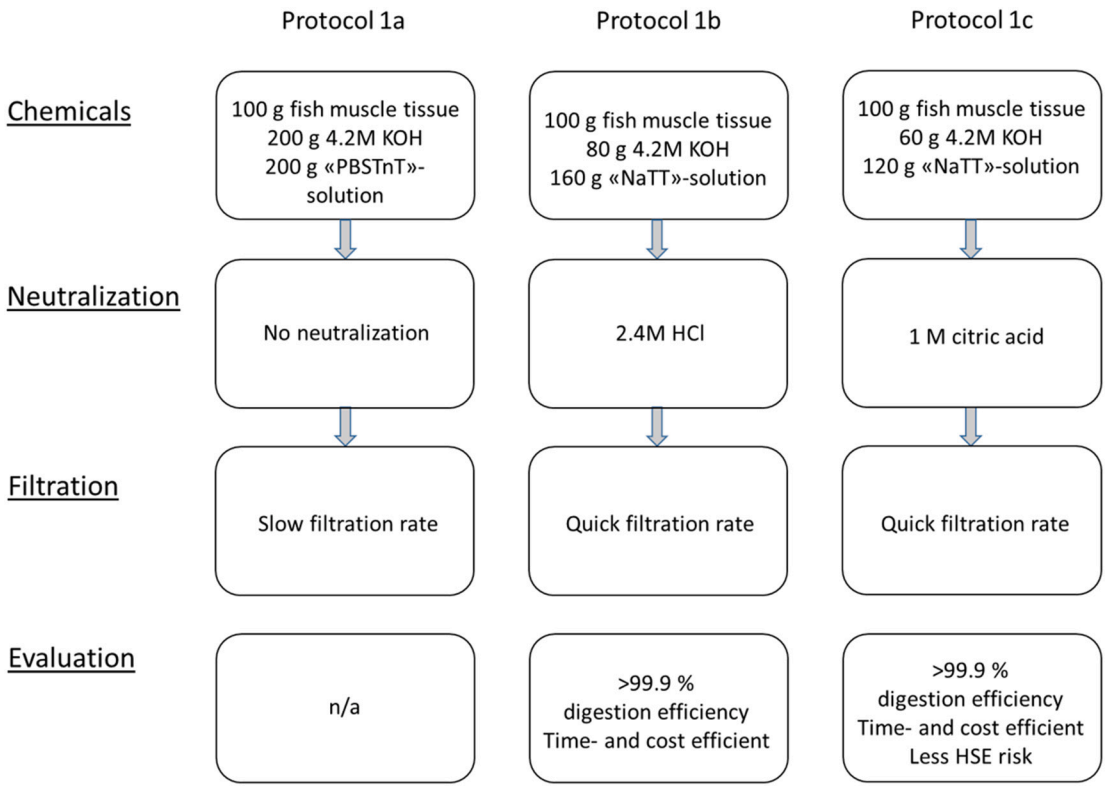

Fig. 1. Flow diagrams of protocols 1a-c, including a short form of the protocols and evaluation. Protocol c was chosen for fish tissue analysis studies in the immediate future.

and 70–88 % for polycarbonate (PC) (Gomiero et al., 2020). PBS solution (with buffering) was used in the initial stages of development to enable a comparison with enzyme digestion. The protocol was later simplified, using a NaCl solution only.

For the current study, 100 g homogenized sample; farmed salmon muscle (or liver or head kidney) was transferred to a 500 ml Erlenmeyer flask. Then 160 g aqueous "NaTT"-solution and 80 g aqueous KOH solution was added, resulting in a 1.4 M KOH solution. The flask was kept in the incubator at 40 °C, and orbitally shaken at 125 rpm for 20–24 h. Then the flask was cooled by an ice-water mixture for 30 min. Aqueous HCl solution was slowly added until pH 7, measured with a LAQUAtwin pocket pH meter (Horiba, Kyoto, Japan) pre-calibrated at pH 4.0, 7.0 and 10.0 using certified Certipur® buffer solutions (Merck KGaA). The solution was heated to 40 °C before filtration, to ease the flow.

Protocol 1c (KOH-"NaTT"-2; graphical abstract): Further incremental changes to the protocol replaced the HCl titration with a more HSE (health, safety and environment)- friendly citric acid, providing an added advantage of being a weak, triprotic acid, with several equivalence points for titration, thus reducing the likelihood of accidentally over-stepping the target pH-value during neutralization. The ratios between matrix, KOH and saline surfactant solution were optimized to reduce the required volume of chemicals.

For the current study, protocol 1c, 100 g homogenized sample was mixed with 120 g NaTT and 60 g 4.2 M KOH, resulting in a 1.4 M KOH solution, which was stirred and incubated at 40 °C for 16-24 h. Thereafter the solution was cooled on ice and neutralized to the indicated pH with citric acid. The solution was heated to 40 °C before filtration. Detailed description in Table S1.

For a summary of the protocols 1a-c, see Fig. 1. In short, protocol 1b resulted in a high DE% and improved filtration rate as compared to protocol 1a. Protocol 1c was further optimized to reduce HSE concerns as well as providing a reduced consumption of chemicals while maintaining the required DE% and filtration rate. For an overview of the ratios of the different chemical components with the matrix, see Table 1.

3.2. *Protocol comparison with published protocols*

The optimized protocol (1c) and the previous protocols (1a and b), with several other published protocols (Protocols 3–7), and KOH only (Protocol 2), were then compared experimentally for their DE%, applied to salmon fillet and some other matrices.

Two oxidative protocols using a) H_2O_2 and HNO_3 (Protocol 3; Bianchi et al., 2020) and b) H_2O_2 with ethanol (Protocol 4; Corami et al., 2020) were tested, as well as two enzymatic protocols using a) Creon® pancrelipase (Protocol 5; von Friesen et al., 2019; Kallenbach et al., 2021), and b) Protamex® (Protocol 6; Liaset et al., 2002) and a combined enzymatic/oxidative protocol using subsequently protease, lipase and H_2O_2 (Protocol 7; Haave et al., 2021). All protocols were carried out as described in the original papers except for protocol 1a-c which were not published before.

Table 1
Relative mass ratio of matrix to mixed solutions and individual chemicals in solution used for the different KOH + saline-surfactant protocols (1a-c).

		Mixed solutions (g)			Individual chemicals in the saline surfactant solutions (g)				
Protocol	Matrix	PBSTnT (aq)	or NaTT (aq)	KOH, 4.2 M (aq)	KOH	Tween®-20	Triton™ X-100	NaCl	KCl, Na_2HPO_4, KH_2PO_4
1a	100 g	200	n/a	200	40	4	2.8	1.6	0.4
1b	100 g	n/a	160	80	16	4.8	3.4	1.4	n/a
1c	100 g	n/a	120	60	12	3.6	2.5	1.1	n/a

When salmon fillet samples were treated with KOH only (protocol 2), filtration was slow and required 1 h 40 min of filtration time. This basic protocol was also tested on other matrices. Some formed a gelatine-like layer that clogged the filter (Fig. S2). With H_2O_2 or enzymes, filtration was difficult (Protocols 4 and 7) or impossible (Protocols 3, 5, 6) using filters with the desired small pore sizes. Furthermore, the enzymatic digestion protocols foremost, and the oxidative digestion protocol second (Protocol 7), involved a considerable sequence of digestion steps that proved both labour intensive and time consuming. None of those protocols were suited for filtration of the digestate of salmon fillet with a filter pore size of 10 μm in our setup. The DE% could not be measured for the protocols that experienced severe clogging during filtration (Protocol 1a, 2, 3, 5, 6) since filtration was abandoned before complete. Among the more successful protocols, Protocol 1b and 1c scored the highest (DE% >99,9), while oxidative protocol 4 scored DE% 85 and the combined enzymatic and oxidative digestion with Protocol 7 scored DE % 91.3–94.4 (mean 93.40 ± 1.54; $N = 5$). These results are summed up in Table 2.

3.3. Improvements by phenomenon

During the time before and during the protocol comparison experiments, incremental improvements were made as described below, sorted by topics:

3.3.1. Fatty fish tissues – improvement by surfactants

Fatty tissues of marine fish like mackerel, salmon, fish liver and oil pose a challenge to digestive polymer isolation protocols. As Lusher et al. (2020) writes, standard alkaline digestion protocols like 1 M KOH are not well suited to such samples. An oily phase may congregate on top of the solution (Fig. S3). This oil layer sometimes clogged the filter, as emulsions of oils and water potentially generate foam. Furthermore, treatment with KOH of some fatty matrices forms viscous semi-solids, resisting filtration. In the experiments, both salmon intestines and a marine oil from pelagic species produced viscous semi-solids during KOH digestion: This semi-solid would not be poured from the Erlenmeyer flask (Fig. S2). In new experiments, the addition of surfactants (Triton™ X-100, Tween®-20) to the digestion of those matrices, made filtration possible. A closer inspection of the two phases revealed that KOH and surfactants together, generated more regularly shaped micelles as compared to those formed in the absence of surfactants (Fig. S3). Tween®-20 and Triton™ X-100 were, from this stage on, added to support the solubilization of fatty matrices. Still, filtration proceeded at a slower pace for fatty matrices than for the less fatty matrices (Fig. S4).

Initial measurements at the full concentrations of Tween®-20 and Triton™ X-100 of Protocol 1a, had shown that the mean filtration time

Table 2
Comparison of our optimized protocol for the digestion of salmon muscle and comparison with other published protocols for biota. Methods 1 a-c were tested on the indicated matrices, protocol 2 on a wider range of samples, and 3–5 on farmed Atlantic salmon.

Protocol number	Short protocol description	Matrix described in study	Incubation temperature, time and amount of tissue	Experience in this study with salmon muscle	Reference
1a	*Surfactants + KOH. No pH neutralization.*	Farmed Atlantic salmon (*Salmo salar*), Haddock (*Melanogrammus aeglefinus*), European plaice (*Pleuronectes platessa*), Atlantic mackerel (*Scomber scombrus*), glacier lantern fish (*Benthosema glaciale*), and European hake (*Merluccius merluccius*). Muscle tissue.	40 °C 16–24 h 100 g	*Matrices appear dissolved. Slow filtration rate.*	*This study*
1b	*Surfactants + KOH combined. pH neutralization by titrating HCl.*	Farmed Atlantic salmon (*Salmo salar*), Haddock (*Melanogrammus aeglefinus*), European plaice (*Pleuronectes platessa*), Atlantic mackerel (*Scomber scombrus*), glacier lantern fish (*Benthosema glaciale*), and European hake (*Merluccius merluccius*). Muscle tissue.	40 °C 16–24 h 100 g	*High DE% (> 99.9 %). Improved filtration rate (*cf. ***1a***).	*This study*
1c	*Surfactants + KOH combined. pH neutralization by titrating citric acid.*	Farmed Atlantic salmon (*Salmo salar*), Haddock (*Melanogrammus aeglefinus*), European plaice (*Pleuronectes platessa*), Atlantic mackerel (*Scomber scombrus*), glacier lantern fish (*Benthosema glaciale*), and European hake (*Merluccius merluccius*). Muscle tissue.	40 °C 16–24 h 100 g	*Reduced use of KOH and surfactants* (cf ***1b***) *without compromising DE% and filtration rate. High DE% (> 99.9 %).*	*This study*
2	*KOH*	American catfish *Clarias gariepinus*. Fish muscle and skin together.	40 °C 16–24 h 5 g in publication 100 g in this study	*Some matrices form gelatinous semisolid. Slow filtration rate.*	Karami et al. (2017)
3	*Acidic oxidative digestion* (H_2O_2/HNO_3)	Atlantic chub mackerel (*Scomber colias)*, European hake (*Merluccius merluccius)*, and Piper gurnard (*Trigla lyra)*. Gastrointestinal tract with its content.	40 °C 12–24 h 3.9–14.3 g in publication 100 g in this study	*Could not filter entire samples at 10* μm. *DE% could not be determined.*	Bianchi et al. (2020)
4	*Oxidative digestion (*H_2O_2, EtOH)	Pacific oysters (*Crassostrea gigas)*. Gills and hepatopancreas.	r.t.-40 °C 24–96 h 0.5 g 100 g in this study	*DE% ~ 85 %.*	Corami et al. (2020)
5	*Enzymatic digestion* Pankreatin (Creon®)	Greenland Smoothcockle (*Serripes groenlandicus)*. Muscle tissue.	37.5 °C 24/48 h 6–35 g in publication 100 g in this study	*Visual residue in solution. Could not filter entire samples at 10* μm. *DE% could not be determined.*	von Friesen et al. (2019)
6	*Enzymatic digestion (*Protamex®)	Atlantic salmon (*S. salar)*. Muscle tissue (fillets).	50 °C 24/48 h 30 g in publication 100 g in this study	*Visual residue in solution. Could not filter entire samples at 10 μm.*	Liaset et al. (2002)
7	*Enzymatic, then oxidative digestion*	Otter (*Lutra lutra*), Sawbill ducks (*Mergus serrator*), common guillemot (*Uria aalge*), Harbor seal (*Phoca vitulina*), Cod (*Gadus morhua*), flounder (*Limanda limanda*). Muscle tissue from each species.	30–50 °C 96 h 6–30 g in publication 100 g in this study	*DE% 91.3–94.4 %. Slow filtration rate.*	Haave et al. (2021)

used for 20 g digested salmon fillet samples were with both detergents present: 39 s ±13, $N = 2$; only Triton™ X-100 present: 46 s ± 28, $N = 3$, only Tween®-20 present 3 min 15 s ± 52 s, N = 2, no detergent present: 1 h 40 min, $N = 1$. To further investigate the role of the surfactants, digestion experiments were carried out with varying concentrations of NaTT with Protocol 1c, including experiments with only Tween®-20 or only Triton™ X-100. KOH and NaCl concentrations were kept constant and the amount of residues on the filters were measured. Although all achieved DE% values, with or without NaTT, were considered good scores for alkaline digestion (DE% >99.9), subtle differences were observed with or without surfactants (Figs. S5 and S6). The presence of surfactants reduced undissolved residues in the filter compared to KOH acting alone. The conclusion from a two-factorial designed experiment, indicated that both Triton™ X-100 and Tween®-20 in the presence of KOH improved the solubilization of salmon muscle. Increasing or decreasing both Triton™ X-100 (from 2.1 to 5 % or to 0.5 %) and Tween®-20 (from 3 to 5 % or to 0.5 %) simultaneously seemed to increase the amount of residues on the filter. Reducing the concentration of Tween®-20 alone had no effect on the amount of residues on the filter (Fig. S5). However, reduction or full absence of Triton™ X-100 increased residues on the filter. A full absence of Tween®-20 lead to increased filtration time and formation of visible aggregates in the solution but did not increase the amount residues on the filter. Assuming the optimized ratio of KOH- and NaTT solution to matrix of 0.6 and 1.2 (Table 1), respectively, as a starting point, different ratios of KOH and NaTT to the matrix salmon fillet were also studied. Doubling the amounts of KOH, or NaTT alone, or both, did not further improve the filtration rate (Fig. S6), on the contrary, doubling of NaTT reduced the filtration rate to 70 %. More striking, however, were the significant negative effects when NaTT was removed from the procedure (Fig. S6).

3.3.2. Suppressing foam with ethanol

Further protocol improvements were implemented to address the excessive amounts of foam that would also resist filtration. It was assumed that the source of the foam were the detergents. A 11.5 M ethanol (*aq*) solution was applied to the foam to reduce the surface tension. Ethanol was also applied if filters ran dry during filtration, as applying further quantities of digested sample solution to a dry filter immediately stopped filtration.

3.3.3. Non-soluble biopolymers

Fish muscle poses unique challenges due to the potential presence of small fragments including mineral-rich bone, cartilage, and fish scales. In a previous project (Gomiero et al., 2020), when a meat mincer was applied to fish fillets in the IMR lab during sample preparation and homogenization, small bone fragments were generated from larger fish bones (Gomiero et al., 2020). After digestion, fragments of fish bone could be seen adhering to the flask walls (Fig. S7). They were fragile after overnight exposure to KOH and difficult to remove mechanically. These biopolymer microparticles (BP) congregate with the MP fraction, potentially overloading filters and occluding MP from subsequent spectro-microscopic identification and quantification. Their composition differs from chitin invertebrate exoskeleton, which can be specifically targeted by chitinase (von Friesen et al., 2019). Thiele et al. (2019) reported similar issues with micro-pearls from bivalve tissues (Thiele et al., 2019), which were also found in our laboratory. From this observation, one could further deduce that sample homogenization based on rotating knives or mincing could potentially also slice MP, and thus affect the size distribution data resulting from the analysis. The BP problem was addressed by adopting a rigorous, time-intensive sample preparation, avoiding/removing bones manually, using tweezers and scalpel. The sample dissection was executed carefully to prevent contamination of the muscle meat with fish scales from the skin. Processing of the fish tissue by a meat mincer as used in previous projects was abandoned. Instead, the fish tissue was cut into roughly 1 cm^3 large chunks with knives on hard wooden trays. The adaption to tissue chunks did not slow down digestion measurably as compared to mincing. If many remaining bones and cartilage or other indigestible tissue parts are observed, those may be removed by sieving the solution (mesh size 1 mm) ~3 h after adding KOH as most of the biological matrix at this point is broken down to a smaller size. Previously, BP fragments were only mentioned by Dehaut et al. (2016) to our knowledge. When digesting samples of the European hake (*Merluccius merluccius*) fillets with skin, a considerable amount of calcium phosphate minerals (apatite), remained undigested as identified by ATR-IR (Fig. S8). These particles totally blocked filtration in a 10 μm pore-size. However, at a pore size of 25 μm, filtration was possible, but still the amounts of mineral collected on the filter were substantial. Such compositions as bone constituents were described before (Dal Sasso et al., 2018) and their dissolution of phosphate minerals in weak solutions of acetic acid or hydrochloric acid (Welch et al., 2002) and calcium carbonate under acidic conditions, e.g. a 0.9 % HCl solution (Rotjan et al., 2019). Most of the minerals were dissolved after a short exposure to a weak HCl solution (1 M, 2 h). However, a separate MP recovery analysis should be undertaken if this step is required.

The Glacier lantern fish is a small mesopelagic fish species, of a few cm length. With fish of this size, it is difficult and impractical to remove bones, skin, cartilage, and intestines. Thus, several approaches were tested: a) digesting the whole fish, b) pre-removal of only the intestines and c) pre-removal of both intestines and head. The filtration of the whole fish digestive solution proved incompatible with a crucible pore size of 10 μm. Filtration was possible after removal of the intestines. However, the DE% was still poor. The most successful filtration and the highest DE% was achieved when both intestines and heads were removed. The results from haddock and glacier lantern fish suggest that, as a minimum, the intestines should be removed from the sample to improve tissue solubilization.

3.3.4. Digestion efficiency

DE%, as in mass loss of sample during the digestion/filtration protocol (see method), could not always be determined precisely due to severe filter clogging, rendering the experiment incomplete (Table 2). In general, most of our experiments involving KOH achieved a DE% >99.9 at pH >7 (Protocol 1b and protocol 1c). This included lean, intermediate and fat fillet samples from haddock, cod, mackerel, and salmon, different organs like liver and head kidney, as well as marine oils (Fig. 2). Visual images of filters at pH 2.5–10.5 are shown in Figs. S9 and S10 for eight of the matrices. Further acidification past pH >7 was not advisable, as the resulting precipitation also clogged the filter. When the dataset of fillets of all four different fish species on for filtration speed were combined and divided into groups of pH 4–6 (mean pH 5.11 ± 0.54, mean DE% 98.43 ± 0.16, $N = 8$), pH 6–9 (mean pH 7.49 ± 0.83, mean DE% 99.63 ± 0.15, $N = 12$) and pH 9–11 (mean pH, 9.61 ± 0.59, mean DE% 99.50 ± 0.06, N = 8) the difference in DE% was significant only between the groups pH 4–6 and pH 6–9 ($p = 0.06$). The differences were less pronounced for the fatty matrices; no significant differences between groups were detected for DE% (Fig. S11). The mean values were for pH 4–7 (mean pH 5.55 ± 0.86, mean DE% 98.34 ± 0.24, $N = 9$), pH 7–9 (mean pH 7.95 ± 0.61, mean DE% 99.27 ± 0.06 $N = 6$) and pH 9–11 (mean pH 9.93 ± 0.29, mean DE% 99.24 ± 0.08 N = 6).

The same tendencies were previously observed in preliminary testing with protocol 1a. The mean DE% for salmon fillet: for pH group 4–6 (mean pH 4.63 ± 0.58), two filters clogged, with a filtration time above two hours, after which time the experiment was abolished. Thus, no average DE% can be provided for this group. The resulting average DE% were for pH 6–9 (mean pH 7.14 ± 1.04, mean DE%, 99.77 ± 0.07, N = 6) and pH 9–11 (99.93 ± 0.01, $N = 4$). In that experiment also haddock fillet and mackerel fillets were tested, at pH 6–7 (mean pH 6.42 ± 0.10, mean DE% 99.98 ± 0.01, $N = 3$; mean pH 6.58 ± 0.44, mean DE%, 99.96 ± 0.01, N = 3, respectively).

In comparison, H_2O_2 in combination with ethanol (Corami et al., 2020), applied on salmon fillet, resulted in a DE% of only ~85 %,

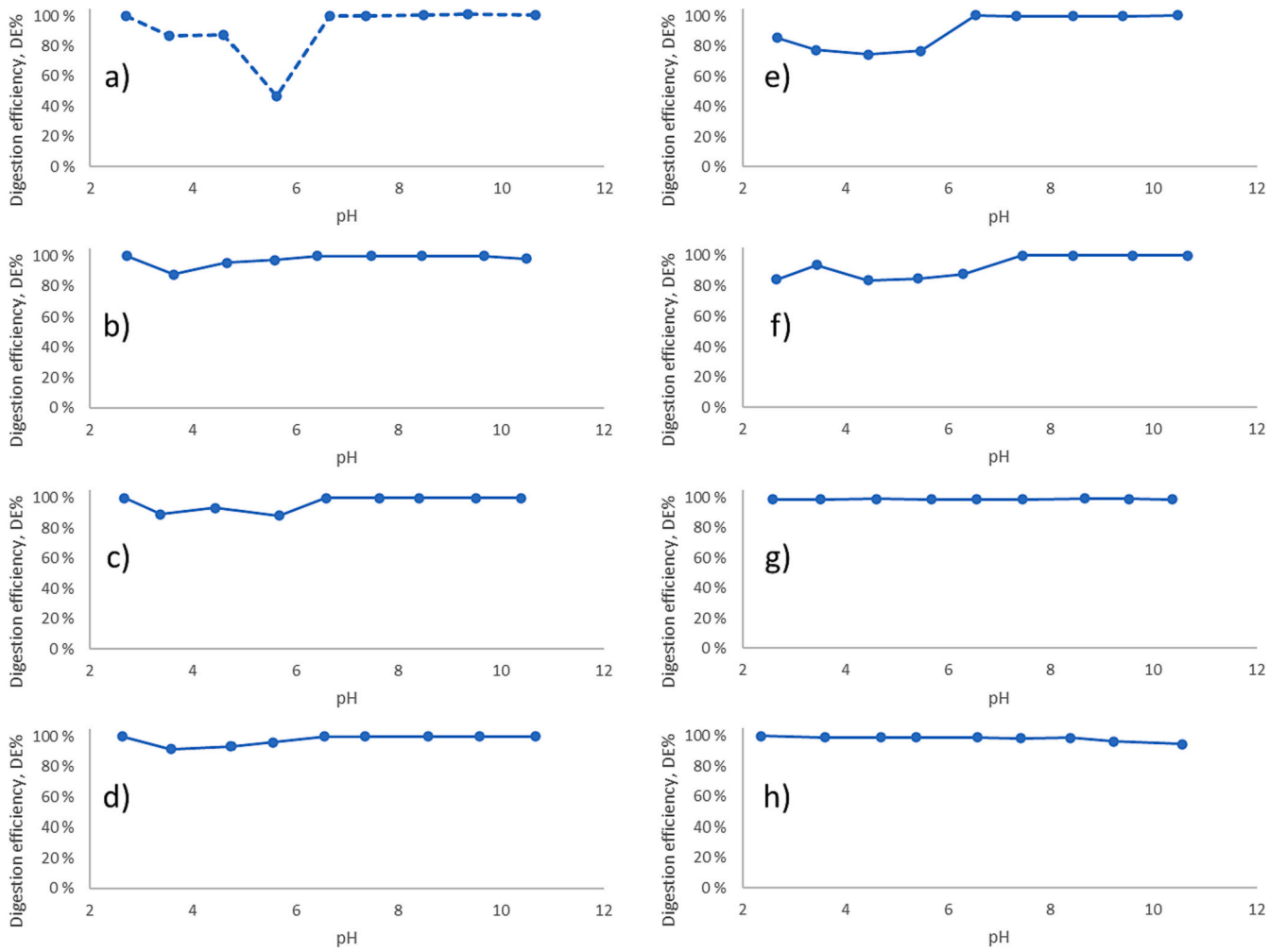

Fig. 2. Screening of pH influence on digestion efficiency (DE%) for different matrices for protocol 1c. DE% for eight different matrices at different pHs. a) Salmon muscle b) Haddock muscle, c) European plaice muscle, d) Cod muscle, e) Salmon liver, f) Salmon head kidney, g) Marine oil pelagic, h) Marine oil meso-pelagic. Not much influence of the pH on the remnants on the DE% was observed.

experiencing filter clogging (Protocol 4, Table 2). Enzymatic, followed by oxidative digestion (Protocol 7, Table 2), worked slightly better, with DE% values between 91.3 and 94.4. However, this amount of residual biological substance rendered subsequent quantitative MP analysis with μFTIR not feasible. Karami et al. (2017) endorsed a 40 °C KOH protocol (Protocol 2, Table 2). To improve DE% to 98.6 for 6 g tissue, an incubation time of 48–72 h was required in addition to a density separation step using aqueous NaI. Later, Süssmann et al. (2021) combined enzymatic treatment using pepsin, with a low concentration of HCl and subsequent incubation with KOH (1:10) (Table 3). In this way, Süssmann et al. (2021) achieved a DE% 99,6 for 10 g tissue with an improved timespan of 16 h incubation. The protocol at hand (1c), is based on a small KOH/matrix ratio with a final concentration of only 1.4 M KOH and a subsequent pH neutralization step, includes surfactants in the reagents mix, thus adapting the protocol for fat-rich marine species with no requirement for enzymes (Figs. 2 and S11). The resulting "clean" filters were found advantageous for subsequent instrumental polymer identification and quantification. Note that fish bones were carefully removed before weighing and digestion of 100 g tissue digestion within 16–24 h. Note also that the achieved advantage in DE% even in the final optimized procedure was just a minor improvement upon already high values in previous studies. While being very influential upon the filtration rate, the DE% values were not in themselves a suitable metric to distinguish the current protocol. The filtration rate however, showed profound differences (Figs. 3 and S11).

3.3.5. *Filters*

In general, the digestates were filtered twice: First to isolate the solid fraction including the analyte MPs. The solid fraction was then flushed off and filtered through a second filter, one that was compatible with the subsequent analytical method. The PTFE-filters were pre-wettened with a few ml ethanol before use. All other filters were pre-wettened with H_2O. For protocol 1a and 1b standard filter crucibles were used. For protocol 1c PTFE filter tiles, cellulose nitrate (CN) filters and stainless-steel filters were also tested. The filter crucibles and PTFE filter tiles were classified as depth filters and the CN as a membrane filter. The stainless-steel filter is a 10 μm mesh sieve covered with a 500 μm mesh sieve for protection and stability. When comparing the performance of ceramic filter crucibles, stainless steel filters, nitrocellulose filters and PTFE filters in combination with our protocol (protocol 1c), the following observations were made: For the filter crucibles, long-term exposure to the alkaline solution proved corrosive, leading to filter disintegration, a weakening the filter's structural integrity. A low recovery rate of 100 μm red PS beads (29 %, where average was 89 % ±4 %), revealed, after close inspection, high counts of fibers and PS beads permanently trapped in the crucible structure, particularly at the edges of the filter, adjacent to the glass wall (Fig. S12). Thus, although new filter crucibles performed well, they may not be well suited for the repeated use required for routine analyses, nor for extended KOH incubation times. Stainless-steel sieves, on the other hand, did not always form a tight seal around the filter edges; particles could slip by the filter

Table 3
Literature comparison of studies investigating methods for digesting fish muscle tissues.

Reference	Species of fish and weight muscle tissue per sample	Reagents Temperature Time	Method	Filter	Digestion efficiency (DE %)	Recovery MP	MP sizes
(Dehaut, Cassone et al. 2016)	Black seabream (*Spondyliosoma cantharus*) Ca. 150 g	KOH (10 %), optional density separation 60 °C, 24 h	Visual, gravimetry, μ-Raman, py-GC–MS	1.6 μm glass fiber (1–2 filters)	99,6–99,8 %	CA degraded, PET shape affected, otherwise no weight changes. Not conclusive for ePS due to low weight. Recovery rate with yellow 500 μm PA-6100 %.	CA, HDPE, LDPE, PA-12, PA-6, PC, PET, PMMA, PP, PS, PSXL, PTFE, PUR, uPVC and ePS: 1–5 mm PA-6: 500 μm
(Karami, Golieskardi et al. 2017)	African catfish (*Clarias gariepinus*) 5 g	KOH (10 %), optional density separation 40 °C, 48–72 h	Visual, gravimetry, Raman analysis	8 μm	98,6 %	PVC slightly degraded (93,3 % R), PET lowered recovery.	LDPE, HDPE, PP, PS, PET, PVC, PA-6, PA-66: 90 % < 300 μm, 10 % < 80 μm
(Süssmann, Krause et al. 2021)	*Lophius piscarorius, pollachius virens, Oncorhynchus keta, Salmo salar, Salmo trutta, Thunnus albacares, Clupea harengus, Renhardtius hippoglossoides, Abguilla Anguilla* 10 g	Pepsin, KOH (10 %) 40 °C, <16 h	Visual, nile red/ fluorescence, py-GC–MS, ATR-FTIR, μ-Raman	1 μm, needed two filters	>99,6 % (when using more than one filter)	Negligible effect on polymers >100 μm, only effect on PAN when assessing with Raman, py-GC–MS and FTIR.	PA-6, PC, PET, PP, PS, PSu, PU: 100–200 μm PA12: 25–50 μm PAN: 50 μm PTFE: 675 μm PVC: 250 μm LDPE: 500 μm PP (red): ≥ 500 μm
Current study	Haddock (*Melanogrammus aeglefinus*), European plaice (*Pleuronectes platessa*), Atlantic mackerel (*Scomber scombrus*), glacier lantern fish (*Benthosema glaciale*), European hake (*Merluccius merluccius*), Atlantic salmon (*Salmo salar*). 100 g	KOH and surfactants 40 °C, 16–24 h	Visual, gravimetry, ATR-FTIR, μ-FTIR,	10 μm	>99,9 %	Tables 4, S2 and S3. Negligible effect on polymers >100 μm. Around 63–80 μm: 50–65 % recovery for PA, PA-66 and PMMA 86–103 % recovery for PE, PP, PS, PVC.	PA-66, PC, PE, PET, PMMA, PP, PS: ~ 3 mm PA-66, PE, PET, PS: 1 mm PA-66, PC, PE, PET, PMMA, PP, PS: 400–500 μm PS, PVC: 100–150 μm PA-66, PC, PE, PMMA, PP, PS, PVC: ca. 63–80 μm

edges, to be lost in the filtrate: Using steel filters lowered recovery rates. The tested cellulose nitrate filters worked well and gave the added practical advantage of being soluble in diluted alkaline solutions, easing the transfer to the second filter (Toto et al., 2023). Ethanol was not used when working with these filters. Issues with clogging of cellulose nitrate filters as described by Süssmann et al. (2021), who applied pepsin digestion combined with a shorter KOH incubation, were not observed (Süssmann et al., 2021). However, samples analyzed by py-GC–MS showed 200–300 % recovery for PVC when cellulose nitrate filters were used. This increase in PVC signal was exclusive for the py-GC–MS measuring technique. The filter material could have contributed to the same pyrolysis products (i.e. benzene) used as quantifiers for PVC. This problem was not observed for μFTIR. It was probably a method-specific misidentification and might be avoided by further developing methods for alternative indicator ion use. This was not pursued in the scope of this project. For the first filtration step, the PTFE tiles were considered the best of the four investigated filter types. These filters could easily be cut to the required size and were handled with tweezers. For the second filtration step, Anodisc filters can be used for both μFTIR and py-GC–MS, which is an advantage. However, their small pore size leads to long filtration times. Furthermore, when sample was applied with a funnel on Anodisc filters, the lighter particles distributed to the filter-rim, and thus were prone to be lost from identification because they stacked on top of each other, or some were outside the scan field applied (Fig. S13). This was prevented by transferring the sample slowly with a pipette. The 5 μm silver filters worked fine for filtration, but for microscopy, the amount of light transmittance was not satisfactory. MP of 80–90 μm could be analyzed easily, but analysis was increasingly problematic with decreasing particle size. When only μFTIR and not py-GC–MS is used, and when there is an ambition for analyzing MP down to 10 μm, Teflon filters with 3 μm pore size worked better.

Generally, in the literature of this field, filter pore size and particle retention are not discussed sufficiently. The goal for MP analysis is a filter pore size fitting the detection limit of the end-point analysis. The filters should be easy to handle, and robust enough to maintain their characteristics during a reasonable number of samples, or cheap enough to be discarded after one use. The duration of the filtration step is closely related to the initial amount of matrix, DE%, pore size and the filter diameter. Adding a density separation such as in Karami et al. (2017) will lead to further particle loss, and increased analysis time and labour. Süssmann et al. (2021) had the ambition for very small filter pores and addressed the clogging issue by using two filters in sequence (1 μm 25 mm) for a 10 g homogenized fillet, increasing both filtration and analysis time. In the current study, to improve filtration speed, large PTFE filters with a pore size of 10 μm were used for the first filtration of the digested sample. Thereafter, the particles on the first filter were transferred to the second, analysis-compatible filter, which had a smaller diameter to reduce the area to be scanned by μFTIR, as a large, scanned area takes considerable time and produces large amounts of data that needs to be stored and analyzed.

3.3.6. *Filtration rate was affected by pH*

Filtration at high pH suffered from excessive foaming, which slowed (muscle tissue) or even stopped filtration (liver and oils), while for low pH, precipitations stopped filtration. Muscle proteins from fish are soluble under both acidic (pH <3) and alkaline conditions (pH >12). However, at pH 5.5, minimum solubility was observed. As much as 80–90 % of the proteins will aggregate and precipitate (Lone et al., 2015; Tian et al., 2017). Precipitation of proteins has a considerable impact on both DE% values and on filtration rate and might increase the chances of misidentifications: FTIR spectra of precipitated fish proteins resemble the spectra for synthetic polyamides (nylons), e.g. PA-66. Especially for

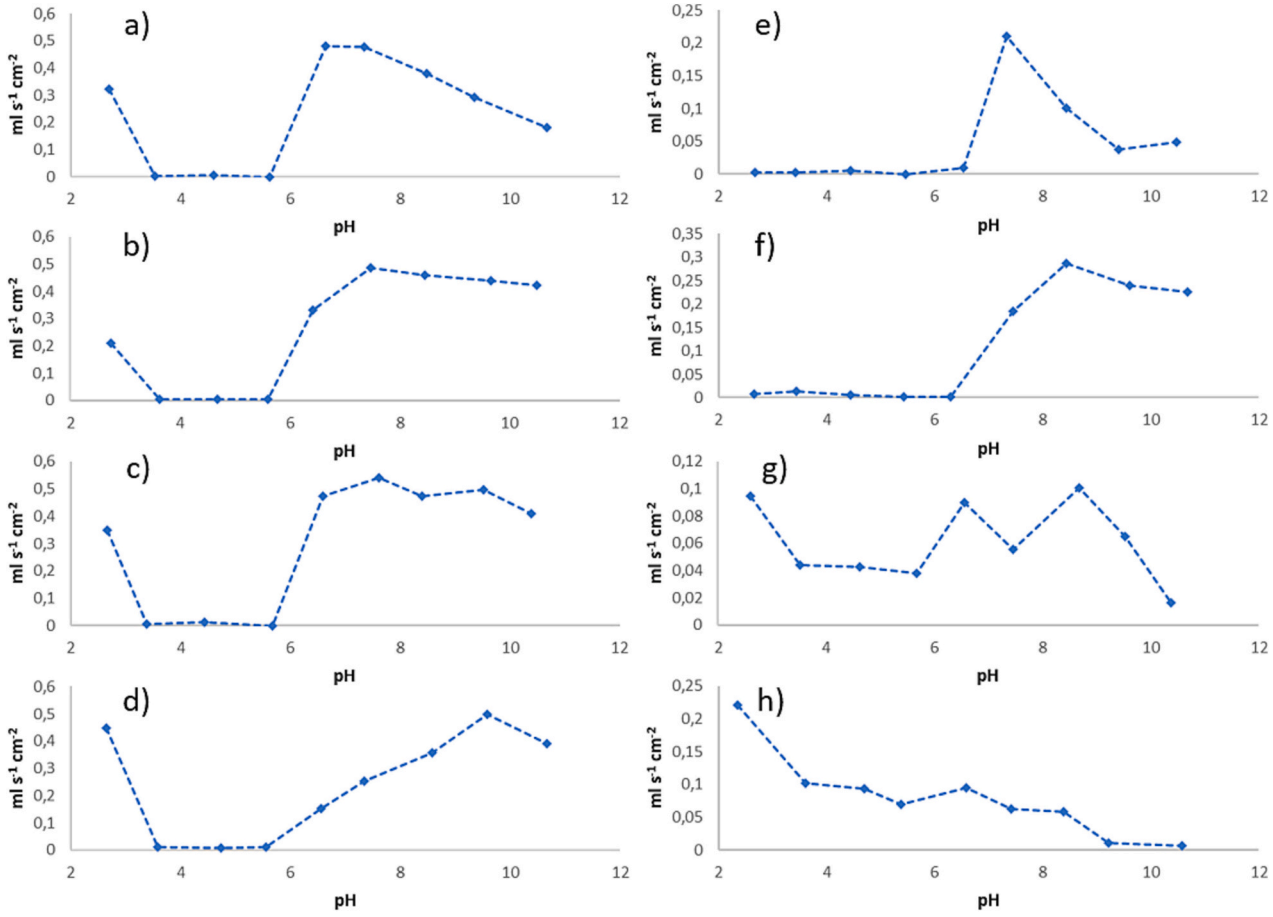

Fig. 3. Screening of pH influence on filtration rates for different matrices for protocol 1c. Different matrices treated with KOH/Natt overnight and titrated to different pHs using citric acid. Corrected filtration rates (y-axis) for different matrices at different pH (x-axis). a) salmon muscle, b) haddock muscle, c) European plaice muscle, d) cod muscle, e) salmon liver, f) salmon head kidney, g) Marine oil pelagic, h) marine oil meso-pelagic. At low pH, filtration was impacted by precipitation, at high pH by foaming.

small particles, for which the signal to noise ratio is higher in FTIR analysis, this can lead to difficulties in matching the acquired spectra with the spectra library and thereby to difficulties in determining the chemical identity. The infrared cut-off at low wavenumbers in an IR spectrometer is around 400 cm^{-1}. In an FPA-μFTIR microscope it is around 900 cm^{-1}, and when using this in combination with Whatman® Anodisc filters, the cut-off is around 1250 cm^{-1} (Primpke et al., 2018), removing part of the comparison area. Fig. S14 compares the ATR-IR spectrum of fish protein isolated at pH 5.5 with that of PA-66. Thus, in FPA-μFTIR, when using Anodisc filters, precipitations of fish proteins could potentially be misidentified as PA-66. The low solubility of fish proteins should be considered, as their presence has a significant negative impact on filtration rate. To test and achieve better filtration rates, the alkaline solution was pH-neutralized, as proposed in Thiele et al. (2019). Both hydrochloric acid (HCl) and citric acid were tested as neutralization agents, and citric acid was preferred as described before. Fig. 3 presents graphs of filtration rates for protocol 1c applied to different matrices treated with KOH/Natt overnight and titrated to different pHs using citric acid. A photographic illustration can be found in Fig. S15. Corrected filtration rates (y-axis) for different matrices at different pH (x-axis). a) salmon muscle (medium fat), b) haddock muscle (medium fat), c) European plaice muscle (low fat), d) cod muscle (low fat), e) salmon liver (high fat), f) salmon head kidney, g) marine oil pelagic, h) marine oil meso-pelagic. Note that most of these curves exhibit a minimum around neutral pH, with pH = 7.5 selected as a compromise for method optimization. As expected, fish muscle samples showed low filtration rates in the range of pH ~3–6 (Figs. 3 and S11). Salmon liver and more so head kidney digestion products had a low filtration rate at pH <7 (Fig. 3, e and f and S11). When the dataset of fillets of all four different fish species for filtration speed were combined and divided into groups (se means of pH under DE% above) of pH 4–6 (mean filtration speed 0.007 ml/s/cm^2 ± 0.005, $N = 8$), pH 6–9 (mean filtration speed 0.486 ml/s/cm^2 ± 0.104, $N = 12$) and pH 9–11 (mean filtration speed 0.467 ml/s/cm^2 ± 0.139, N = 8), the pH 4–6 group was significantly different from both the other groups ($p = 0.003$ and 0.004), while for the fatty matrices (liver and oils) in groups of pH 4–7 (mean filtration speed 0.067 ml/s/cm^2 ± 0.046, $N = 9$), pH 7–9 (mean filtration speed 0.561 ml/s/cm^2 ± 0.059, $N = 6$) and pH 9–11 (mean filtration speed 0.059 ml/s/cm^2 ± 0.016 N = 6), the pH 7–9 group was significantly different from both other groups ($p = 0.06$ and 0.004) (Fig. S11). The same tendencies were previously observed in preliminary testing with protocol 1a, in which, however, the data was not corrected for filter performance. The mean filtration speeds for salmon fillet: for pH group 4–6, two filters clogged, so the filtration time exceeded 2 h. For the calculation of mean values, those filtrations were attributed to the maximum value of 2 h. The resulting average filtration rates were for pH 4–6 (mean filtration speed 0.008 ml/s/cm^2 ± 0.008, $N = 4$), pH 6–9 (mean filtration speed 0.783 ml/s/cm^2 ± 0.021, N = 6) and 9–11 (mean filtration speed 0.843 ml/s/cm^2 ± 0.522, N = 8). In that set of experiments haddock fillet and mackerel fillet were tested at pH 6–7 (haddock: mean pH 6.42 ± 0.10, mean filtration speed 0.049 ml/s/cm^2 ± 0.013, $N = 3$; mackerel: mean pH 6.58 ± 0.44, mean filtration speed 0.044 ml/s/cm^2 ± 0.016, N = 3). One marine oil did not suffer from protein precipitation (Fig. 3h).

The above-mentioned optimal pH ranges should not be considered a generalized "fit for all" procedure: Due to biological variability, the optimal pH will vary from sample to sample. Thus, in practice, we apply the sample on the filter, with the vacuum pump active, and then adjust pH with citric acid until the sample flows. Sometimes, the optimal pH is overrun. This is corrected for with careful addition of a little concentrated KOH. In this procedure, however, it is helpful to know at which pH a flow is to be expected.

With foam suppression using ethanol, and with carefully maintaining a liquid layer in the filter to prevent air penetration, filtration of the neutralized sample solution achieved a considerable filtration rate improvement from at worst >6 h to <5 min. However, individual samples can occasionally suffer from filtration times of >1 h, due to so far unidentified biological variations. The optimization was incorporated in protocol 1c.

3.3.7. Sample size

There is no reason to expect a uniform distribution of MP in fish tissue, not even in the muscle tissue, as the character and composition of the muscle varies with its function (Nortvedt and Tuene, 1998). Therefore, larger samples are required to represent the contamination in the fillet. The proposed method is for routine analysis of 100 g fish muscle per sample, an amount which is more representative of the fish than other methods mentioned in literature (Table 3) except for Dehaut et al. (2016), who used ca. 150 g per sample. However, for the 150 g samples, as described by Dehaut et al. (2016), two filters were used, and the filters were slightly loaded. Thus, additional sample treatment steps may be required for the isolated solid matter to be applicable for subsequent instrumental analysis. Incubation with KOH at the higher temperature of 60 °C has been reported to degrade polymers such as PET (Karami et al., 2017), and thus should be avoided. The two other methods used 5 g (Karami et al., 2017) and 10 g (Süssmann et al., 2021) fish muscle. The current method is cheaper, while providing temperature, time consumption and DE% values, comparable to the method published by Süssmann et al. (2021) yet works for a larger sample size.

3.3.8. Polymer damage and recovery

Recognizing the requirement for the fish matrix digestion protocol to preserve MP quantitatively, MP of selected polymer types were exposed to the optimized protocol for an assessment of vulnerability. The pre- and post-protocol status of the exposed particles were analyzed for MP of eight common polymer types (PA-66, PC, PE, PET, PMMA, PP, PS and PVC) in different particle sizes. Polymer damage was evaluated depending on the particle size by visual inspection under a microscope, gravimetric analysis, ATR-IR, counting of particles, determination of particle size and area under LED/UV-LED digital microscope or by μFTIR microscope. The results are described below.

Seven MP polymer types of particle size ~3 mm, were assayed visually under a microscope and gravimetrically before and after the exposure to protocols 1a-c. In addition, the ATR-IR spectra of the surface of the particles were studied. Visual post-protocol inspection under the microscope using LED and UV-LED light, revealed no observable corrosive effect. The largest pre- and post-protocol mass difference, observed for PC, corresponds to <0.5 % mass loss during exposure (Table S2). Thus, both mass difference and the microscope assay suggest a negligible level of procedural polymer corrosion. PCA multivariate analysis was used to identify more subtle effects. It was applied to the FTIR spectral data. While not directly transferable to the MP quantification results, PCA may be indicative of qualitative molecular changes in the polymer surface. For PA-66, the polymer with the least observed mass loss effect (0.01 % mass loss), the FTIR spectrum changed intensity in peaks at wavelengths of 2850 and 2920 cm^{-1}. New peaks in the spectrum were found for the polymers HDPE, LDPE, PP and PS. These peaks correlated with peaks in the spectrum library for Triton™X-100 and Tween20®. The possible Triton-X-100 and Tween-20 peaks in the spectra, persistent after additional washing, may suggest at least a moderate sorption of the detergents, potentially opposing a weight loss due to polymer corrosion. However, other library peaks at 1510 and 1250 cm^{-1} were absent. These peaks would be expected if the spectra reflected an adsorption of Triton and Tween mixtures to the MP. According to Richardson and Meakin, 1974, adsorption of surfactants increases with higher pH (Richardson and Meakin, 1974). A new peak at 1750 cm^{-1} could not be explained. Additional washing and drying of the particles did not change the spectra. No conclusion could be drawn from these observations.

Regarding MP particle size change, seven different polymer type fragments in the size range 400–500 μm (PA-66, PC, PE, PET, PMMA, PP, PS) and PVC of 150 μm were exposed to protocol 1b. Recovery was good or acceptable (>70 %) for all polymers (Table S3). The observed increase in particle size variation was in most cases likely due to the more complex task of manually separating the particles after treatment, as compared to the clean and dry particles before. Particle size changes (%) were − 11 (PMMA), −10 (PC), −5 (PP), 0 (PA), 0 (PE), 0 (PET), +2.5 (PVC) and + 6 (PS), respectively. For PC, the polymer type with the highest mass loss, this was likely explained by polymer chain disruption by KOH. The surface of PMMA felt sticky after only one treatment, which was likely due to the post-procedure cleaning /drying with Ethanol 96 %. Recovery rates (%) were 96 (PE), 88 (PA), 87.5 (PET), 84 (PS), 83.5 (PVC), 81 (PP), 79 (PC) and 74 (PMMA) on average (Table S3). Smaller particles of PVC (160 μm) and PS (100 μm) were recovered on average with 80 % for PVC and 89 % for PS. Note that for PVC an increase in particle size (3 %) was observed. Speculatively, swelling of the surface layer from liquid penetration into the polymer structure might explain this phenomenon. Recovery of red PS beads of 100 μm from matrix was 89 and 83 % for salmon fillet and 86 and 92 % for salmon liver.

Finally, to study effects on smaller particles, as they have a larger surface to volume ratio and hence should be more vulnerable for digestion, cryo-milled particles from eight polymer types were sieved with pore sizes 63 and 80 μm. The goal was to collect particles within this size range. The collected particles were measured for size with μFTIR. The results indicated a deviation from the target range for PMMA and PA-66 towards smaller particles, and for PC towards larger particles (Fig. S1). They were then exposed to protocol 1c (Table S4) in three parallels. Recoveries for PE, PP, PS and PVC were > 86 %, for PET 75 %, PMMA 65 %, PA-66 60 % and 53 % for PC on average (Table 4).

Ideally, the protocol conditions heat, and corrosiveness should not damage target polymer types. MP tested for recovery should ideally cover the complete size and polymer type spectrum analyzed, as relative procedural damage is inversely related to particle size. Thus, digestion may lead to significant size reductions with MP originally close to the targeted minimum MP size. The smallest collected particles may originally have been larger before exposure to the analytical conditions, and particles originally close to the filter pore size may be lost through the filter. Hence, the generated analytical data size-distribution results are potentially affected to an unknown degree for the smallest particles.

Süssmann et al. (2021), who employed a combination of pepsin and KOH at 40 °C achieved >90 % recovery of all MP of PA, PC, PE, PET, PP,

Table 4
Recovery percentage with protocol 1c. In triplicates, MP of size ranges around 63–80 μm (see Fig. S1) were applied on Anodisc filters and analyzed by μFTIR. Anodisc filters were dissolved (see Methods) and the product was added a new filter, followed by μFTIR analysis.

Recovery %	Test 1	Test 2	Test 3	mean	STDEV
PE	85	75	99	86	12.1
PP	94	82	114	97	16.2
PS	101	97	111	103	7.2
PVC	93	81	112	95	15.6
PET	55	92	79	75	18.8
PC	26	72	62	53	24.2
PA-66	58	64	58	60	3.5
PMMA	36	93	67	65	28.5

PS, PSu, PTFE, PU and PVC of 100–200 μm, indicative of negligible polymer corrosion. In the study at hand, acceptable recoveries for MP of 100–500 μm of 80–96 % for PA, PE, PET, PS, PVC and PP were found. For PC and PMMA recoveries for this size class were lower: 70–80 %. For even smaller particles, 63–80 μm, recoveries were 53–100 %, depending on the polymer type (Table 4). The recovery numbers of Süssmann et al. (2021) referred to their protocol for lean fish tissues with a short incubation in KOH of 4 h, which was not suited for fatty matrices. For those, Süssmann et al. present a prolonged hydrolysis of 16 h without presenting recoveries for that protocol, which might explain the discrepancies.

Overall, the FTIR data supports that the investigated protocol preserves the chemical integrity of the examined polymer types / MP size range to an extent required for the purpose of a monitoring program. However, limitations should be kept in mind when interpreting the data.

3.4. Limitations

Measurement uncertainties will change with polymer types and particle sizes due to increased vulnerability of smaller particles. For MP of sizes approaching the filter pore size (10 μm), the measurement uncertainty due to particle loss is expected to be high. The current experiments were not suited for reliable measurement uncertainty estimates in that size range, as our own produced recovery test material (playing around 63–80 μm), did not cover that size spectrum well. No such material is available for purchase. Emulsion polymerized MP that are often used as recovery material of smaller sizes is commercially available. However, their shape is not comparable to the bulk of environmental MP which are fragments, foils or fibers. The in-house generated MP materials were considered a better model system for recovery and vulnerability experiments.

One should keep in mind that MP of polymer types not included in the study, and MP of sizes below the above-mentioned recovery experiments, all will be affected to an unknown degree. Furthermore, polymer production specifics such as different additives may potentially affect the MP vulnerability. The current study design did not address this issue.

The optimized protocol, and probably most published methods, will extract and isolate present BP micro-particles together with the MP. Care should be taken to ensure removal of BP generating material prior to all analytical steps that could generate BP micro-particles. These would otherwise be retained in the filter with the analyte MP fraction, clogging filters, potentially occluding the (often fewer) extracted analyte MP, as well as interfering with and potentially invalidating a subsequent μFTIR measurement as well as light microscopic MP assay. Even though some BP can be readily identified with μFTIR, they can be hard to distinguish visually from MP and may interfere with py-GC–MS by producing the same indicator ions that are used for the quantification of MP. A careful selection of qualifier and quantifier ions is required to prevent misidentifications (Fischer and Scholz-Bottcher, 2017).

Marine samples are characterized by a diversity of tissue types. This method was not suited for the digestion of the gastrointestinal tract with content, nor for the heads of fishes. For fishes consumed whole and for the analysis of the content of the gastrointestinal tract, other methods should be employed. Tissues other than those tested may present new challenges.

4. Conclusion

A quick and efficient digestion protocol to solubilize fatty and lean fish fillets, fish livers and oils for MP analysis was developed. The protocol is based on surfactant aided alkaline (KOH) digestion and subsequent vacuum filtration after pH-adjustment to neutral, aided by surface tension reduction using ethanol to suppress foam. The required man hours, dominated by the filtration step, and by the total number of procedural steps, were reduced relatively to other protocols, thus providing an analytical capacity for a higher number of samples as required for monitoring and surveillance purposes. The DE% was above 99.9 % for most matrices. While this improvement was an asset for filtration and for subsequent polymer quantification, DE% was not in itself able to distinguish the proposed protocol. The protocol improved upon common issues with seafood digestive protocols and general protocols applied to seafood: The ability to successfully digest fat rich tissues, reduce filter-clogging and foam-generation, yielding an improved, acceptable filtration speed. An issue with generation and subsequent *co*-extraction of bio-polymer micro particles was identified. It was addressed by a careful removal of fish bones and skin. Homogenization by food processor or meat mincing was removed from the procedure: Digestion was instead carried out on ~1 cm^3 knife-cut chunks of the samples. This procedure will also protect the MP from exposure to the rotating knife, which potentially could alter the size-distribution of the MP towards smaller particles and from contamination though plastic parts from parts of the instrument used for homogenization. The seafood tissue inhomogeneity issues were addressed by an analytical capacity for a large sample analysis, unmatched by most published MP analytical protocols.

Regarding polymer vulnerability: PC, PA and PMMA particles of the smallest examined size range were recovered with significant but acceptable levels of mass loss. Measurement uncertainty in this size range is elevated, as is common in analytical chemistry for results close to the Limit of Quantification. In contrast, PE, PP, PS and PVC, and PET proved more resistant, also in the smallest examined size range. The larger particles in all polymer types, were, as could be expected, more robust to the procedural conditions than smaller particles of the same polymer.

One lesson from this study is that the more a specific matrix is targeted, e.g. only muscle, or only liver etc., the more likely a successful, quick, high DE% and low residue protocol can be developed. Finally, some of the tested filters proved vulnerable to the procedure, leading to a loss of MP.

Funding

This work was funded by the Norwegian Ministry of Trade, Industry and Fisheries, Institute of Marine Research project 15293. Marine oils from pelagic and mesopelagic species were provided from the ongoing research project MEESO (EU H2020 research and innovation program, Grant Agreement No 817669) at the IMR.

CRediT authorship contribution statement

Helge Torbjørn Bull Hove: Conceptualization, Data curation, Formal analysis, Investigation, Methodology, Supervision, Writing – original draft, Writing – review & editing. **Thomas Næsheim:** Conceptualization, Data curation, Formal analysis, Investigation, Methodology, Visualization, Writing – original draft, Writing – review & editing. **Tanja Kögel:** Conceptualization, Data curation, Formal analysis, Investigation, Methodology, Visualization, Funding acquisition, Project administration, Supervision, Writing - original draft, Writing - review & editing.

Declaration of competing interest

The authors declare the following financial interests/personal relationships which may be considered as potential competing interests: Tanja Koegel reports financial support was provided by Norwegian Ministry for Trade, Industry and Fisheries. Tanja Koegel reports a relationship with Netherlands Organization for Health Research and Development that includes: consulting or advisory. Thomas Næsheim is currently employed at EUROFINS, carrying out microplastic analysis.

Data availability

Data will be made available on request.

Acknowledgements

With grief we learned that our friend and co-author of this paper, Ørjan Bjorøy, unexpectedly and abruptly died on January 29, 2022. He was involved in this manuscript on the level of a co-author in conceptualization, investigation, validation, analysis, and writing. Ørjan was a good person, an excellent analyst, and a knowledgeable scientist. Our memories of him are precious to us and he is sincerely missed.

We thank Anders Fuglevik, Felicia Couillard and Stig Valdersnes (IMR) for practical laboratory work and method development discussions. André Bienfait and Alice Refosco (IMR) for providing cryo-milled and sieved material in the size range of 63-80 μm and AR for critical comments on the manuscript. Aina Bruvik and Nawaraj Gautam (IMR) for preparing the fish tissue samples used in the study and the personnel of the Institute of Marine Research's reference fleet and the research vessels for their assistance in collecting fish samples. We thank Svein Mjøs (University of Bergen) for discussions and help with the experimental design studies.

Appendix A. Supplementary data

Supplementary data to this article can be found online at https://doi.org/10.1016/j.marpolbul.2023.115726.

References

Atugoda, T., Vithanage, M., Wijesekara, H., Bolan, N., Sarmah, A.K., M. S. Bank, You, S. M., Ok, Y.S., 2021. Interactions between microplastics, pharmaceuticals and personal care products: implications for vector transport. Environ. Int. 149, 106367 https://doi.org/10.1016/j.envint.2020.106367.

Avio, C.G., Gorbi, S., Regoli, F., 2015. Experimental development of a new protocol for extraction and characterization of microplastics in fish tissues: first observations in commercial species from Adriatic Sea. Mar. Environ. Res. 111, 18–26. https://doi.org/10.1016/j.marenvres.2015.06.014.

Bai, C.L., Xu, T.T., Guo, Y., Li, H.T., 2022. A rapid method for extracting microplastics from oily food samples. Anal. Methods 14 (36), 3529–3538. https://doi.org/10.1039/d2ay00792d.

Bianchi, J., Valente, T., Scacco, U., Cimmaruta, R., Sbrana, A., Silvestri, C., Matiddi, M., 2020. Food preference determines the best suitable digestion protocol for analysing microplastic ingestion by fish. Mar. Pollut. Bull. 154, 111050 https://doi.org/10.1016/j.marpolbul.2020.111050.

Bodzon-Kulakowska, A., Bierczynska-Krzysik, A., Dylag, T., Drabik, A., Suder, P., Noga, M., Jarzebinska, J., Silberring, J., 2007. Methods for samples preparation in proteomic research. J. Chromatogr. B Anal. Technol. Biomed. Life Sci. 849 (1–2), 1–31. https://doi.org/10.1016/j.jchromb.2006.10.040.

Budimir, S., Setala, O., Lehtiniemi, M., 2018. Effective and easy to use extraction method shows low numbers of microplastics in offshore planktivorous fish from the northern Baltic Sea. Mar. Pollut. Bull. 127, 586–592. https://doi.org/10.1016/j.marpolbul.2017.12.054.

Catarino, A.I., Thompson, R., Sanderson, W., Henry, T.B., 2017. Development and optimization of a standard method for extraction of microplastics in mussels by enzyme digestion of soft tissues. Environ. Toxicol. Chem. 36 (4), 947–951. https://doi.org/10.1002/etc.3608.

Claessens, M., Van Cauwenberghe, L., Vandegehuchte, M.B., Janssen, C.R., 2013. New techniques for the detection of microplastics in sediments and field collected organisms. Mar. Pollut. Bull. 70 (1–2), 227–233. https://doi.org/10.1016/j.marpolbul.2013.03.009.

Client_Earth, 2021. Analysis of intentionally-added microplastics' emissions to the environment up to 2030. In: European Environmental Bureau (EEB).

Cole, M., Webb, H., Lindeque, P.K., Fileman, E.S., Halsband, C., Galloway, T.S., 2014. Isolation of microplastics in biota-rich seawater samples and marine organisms. Sci. Rep. 4, 4528 https://doi.org/10.1038/srep04528.

Corami, F., Rosso, B., Roman, M., Picone, M., Gambaro, A., Barbante, C., 2020. Evidence of small microplastics (< 100 mu m) ingestion by Pacific oysters (Crassostrea gigas): a novel method of extraction, purification, and analysis using Micro-FTIR. Mar. Pollut. Bull. 160, 111606 https://doi.org/10.1016/j.marpolbul.2020.111606.

Courtene-Jones, W., Quinn, B., Murphy, F., Gary, S.F., Narayanaswamy, B.E., 2017. Optimisation of enzymatic digestion and validation of specimen preservation methods for the analysis of ingested microplastics. Anal. Methods 9 (9), 1437–1445. https://doi.org/10.1039/c6ay02343f.

Dal Sasso, G., Asscher, Y., Angelini, I., Nodari, L., Artioli, G., 2018. A universal curve of apatite crystallinity for the assessment of bone integrity and preservation. Sci. Rep. 8 (1), 12025. https://doi.org/10.1038/s41598-018-30642-z.

Dehaut, A., Cassone, A.L., Frere, L., Hermabessiere, L., Himber, C., Rinnert, E., Riviere, G., Lambert, C., Soudant, P., Huvet, A., Duflos, G., Paul-Pont, I., 2016. Microplastics in seafood: benchmark protocol for their extraction and characterization. Environ. Pollut. 215, 223–233. https://doi.org/10.1016/j.envpol.2016.05.018.

Ding, J.N., Zhang, S.S., Razanajatovo, R.M., Zou, H., Zhu, W.B., 2018. Accumulation, tissue distribution, and biochemical effects of polystyrene microplastics in the freshwater fish red tilapia (Oreochromis niloticus). Environ. Pollut. 238, 1–9. https://doi.org/10.1016/j.envpol.2018.03.001.

Enders, K., Lenz, R., Beer, S., Stedmon, C.A., 2017. Extraction of microplastic from biota: recommended acidic digestion destroys common plastic polymers. ICES J. Mar. Sci. 74 (1), 326–331. https://doi.org/10.1093/icesjms/fsw173.

Fischer, M., Scholz-Bottcher, B.M., 2017. Simultaneous trace identification and quantification of common types of microplastics in environmental samples by pyrolysis-gas chromatography-mass spectrometry. Environ. Sci. Technol. 51 (9), 5052–5060. https://doi.org/10.1021/acs.est.6b06362.

Foekema, E.M., De Gruijter, C., Mergia, M.T., van Franeker, J.A., Murk, A.J., Koelmans, A.A., 2013. Plastic in North Sea fish. Environ. Sci. Technol. 47 (15), 8818–8824. https://doi.org/10.1021/es400931b.

von Friesen, L.W., Granberg, M.E., Hassellov, M., Gabrielsen, G.W., Magnusson, K., 2019. An efficient and gentle enzymatic digestion protocol for the extraction of microplastics from bivalve tissue. Mar. Pollut. Bull. 142, 129–134. https://doi.org/10.1016/j.marpolbul.2019.03.016.

Gomiero, A., Haave, M., Bjorøy, Ø., Herzke, D., Kögel, T., Nikiforov, V., Øysæd, K.B., 2020. Quantification of Microplastic in Fillet and Organs of Farmed and Wild Salmonids- a Comparison of Methods for Detection and Quantification. NORCE Miljø.

Groh, K.J., Backhaus, T., Carney-Almroth, B., Geueke, B., Inostroza, P.A., Lennquist, A., Leslie, H.A., Maffini, M., Slunge, D., Trasande, L., Warhurst, A.M., Muncke, J., 2019. Overview of known plastic packaging-associated chemicals and their hazards. Sci. Total Environ. 651, 3253–3268. https://doi.org/10.1016/j.scitotenv.2018.10.015.

Grosvik, B.E., Granberg, M.E., Kogel, T., Lusher, A.L., Gomiero, A., Halldorsson, H.P., Madsen, A.K., Baak, J.E., Guls, H.D., Magnusson, K., 2022. Microplastics in Arctic invertebrates: status on occurrence and recommendations for future monitoring. Arctic Sci. https://doi.org/10.1139/as-2022-0004.

Haave, M., Gomiero, A., Schonheit, J., Nilsen, H., Olsen, A.B., 2021. Documentation of microplastics in tissues of wild coastal animals. Front. Environ. Sci. 9, 575058 https://doi.org/10.3389/fenvs.2021.575058.

Hermsen, E., Mintenig, S.M., Besseling, E., Koelmans, A.A., 2018. Quality criteria for the analysis of microplastic in biota samples: a critical review. Environ. Sci. Technol. 52 (18), 10230–10240. https://doi.org/10.1021/acs.est.8b01611.

Isobe, A., Buenaventura, N.T., Chastain, S., Chavanich, S., Cozar, A., DeLorenzo, M., Hagmann, P., Hinata, H., Kozlovskii, N., Lusher, A.L., Marti, E., Michida, Y., Mu, J.L., Ohno, M., Potter, G., Ross, P.S., Sagawa, N., Shim, W.J., Song, Y.K., Takada, H., Tokai, T., Torii, T., Uchida, K., Vassillenko, K., Viyakarn, V., Zhang, W.W., 2019. An interlaboratory comparison exercise for the determination of microplastics in standard sample bottles. Mar. Pollut. Bull. 146, 831–837. https://doi.org/10.1016/j.marpolbul.2019.07.033.

Kallenbach, E.M.F., Hurley, R.R., Lusher, A., Friberg, N., 2021. Chitinase digestion for the analysis of microplastics in chitinaceous organisms using the terrestrial isopod Oniscus asellus L. as a model organism. Sci. Total Environ. 786, 147455 https://doi.org/10.1016/j.scitotenv.2021.147455.

Karami, A., Golieskardi, A., Choo, C.K., Romano, N., Bin Ho, Y., Salamatinia, B., 2017. A high-performance protocol for extraction of microplastics in fish. Sci. Total Environ. 578, 485–494. https://doi.org/10.1016/j.scitotenv.2016.10.213.

Karlsson, T.M., Vethaak, A.D., Almroth, B.C., Ariese, F., van Velzen, M., Hassellov, M., Leslie, H.A., 2017. Screening for microplastics in sediment, water, marine invertebrates and fish: method development and microplastic accumulation. Mar. Pollut. Bull. 122 (1–2), 403–408. https://doi.org/10.1016/j.marpolbul.2017.06.081.

Kogel, T., Rudolf, R., Hodneland, E., Copier, J., Regazzi, R., Tooze, S.A., Gerdes, H.H., 2013. Rab3D is critical for secretory granule maturation in PC12 cells. PLoS One 8 (3), e57321. https://doi.org/10.1371/journal.pone.0057321.

Kögel, T., Refosco, A., Maage, A., 2020. Surveillance of seafood for microplastics. In: Teresa Rocha-Santos, M.C., Mouneyrac, Catherine (Eds.), Handbook of Microplastics in the Environment. Springer Link. https://doi.org/10.1007/978-3-030-10618-8_28-1.

Kogel, T., Hamilton, B.M., Granberg, M.E., Provencher, J., Hammer, S., Gomiero, A., Magnusson, K., Lusher, A.L., 2022. Current efforts on microplastic monitoring in Arctic fish and how to proceed. Arctic Sci. https://doi.org/10.1139/as-2021-0057.

Kuhn, S., van Werven, B., van Oyen, A., Meijboom, A., Rebolledo, E.L.B., van Franeker, J. A., 2017. The use of potassium hydroxide (KOH) solution as a suitable approach to isolate plastics ingested by marine organisms. Mar. Pollut. Bull. 115 (1–2), 86–90. https://doi.org/10.1016/j.marpolbul.2016.11.034.

Liaset, B., Nortvedt, R., Lied, E., Espe, M., 2002. Studies on the nitrogen recovery in enzymic hydrolysis of Atlantic salmon (Salmo salar, L.) frames by Protamex (TM) protease. Process Biochem. 37 (11), 1263–1269. https://doi.org/10.1016/S0032-9592(02)00003-1.

Lone, D.A., Wani, N.A., Wani, I.A., Masoodi, F.A, 2015. Physico-chemical and functional properties of Rainbow trout fish protein isolate. Int. Food Res. J. 22 (3), 1112–1116.

Loder, M.G.J., Imhof, H.K., Ladehoff, M., Loschel, L.A., Lorenz, C., Mintenig, S., Piehl, S., Primpke, S., Schrank, I., Laforsch, C., Gerdts, G., 2017. Enzymatic purification of microplastics in environmental samples. Environ. Sci. Technol. 51 (24), 14283–14292. https://doi.org/10.1021/acs.est.7b03055.

Lusher, A.L., Welden, N.A., Sobral, P., Cole, M., 2017. Sampling, isolating and identifying microplastics ingested by fish and invertebrates. Anal. Methods 9 (9), 1346–1360. https://doi.org/10.1039/c6ay02415g.

Lusher, A.L., Munno, K., Hermabessiere, L., Carr, S., 2020. Isolation and extraction of microplastics from environmental samples: an evaluation of practical approaches and recommendations for further harmonization. Appl. Spectrosc. 74 (9), 1049–1065. https://doi.org/10.1177/0003702820938993.

Miller, M.E., Kroon, F.J., Motti, C.A., 2017. Recovering microplastics from marine samples: a review of current practices. Mar. Pollut. Bull. 123 (1–2), 6–18. https://doi.org/10.1016/j.marpolbul.2017.08.058.

Mintenig, S.M., Int-Veen, I., Loder, M.G.J., Primpke, S., Gerdts, G., 2017. Identification of microplastic in effluents of waste water treatment plants using focal plane array-based micro-Fourier-transform infrared imaging. Water Res. 108, 365–372. https://doi.org/10.1016/j.watres.2016.11.015.

Munno, K., Helm, P.A., Jackson, D.A., Rochman, C., Sims, A., 2018. Impacts of temperature and selected chemical digestion methods on microplastic particles. Environ. Toxicol. Chem. 37 (1), 91–98. https://doi.org/10.1002/etc.3935.

Munyaneza, J., Jia, Q.L., Qaraah, F.A., Hossain, M.F., Wu, C.Z., Zhen, H.J., Xiu, G.L., 2022. A review of atmospheric microplastics pollution: in-depth sighting of sources, analytical methods, physiognomies, transport and risks. Sci. Total Environ. 822, 153339 https://doi.org/10.1016/j.scitotenv.2022.153339.

Naidoo, T., Goordiyal, K., Glassom, D., 2017. Are nitric acid (HNO3) digestions efficient in isolating microplastics from juvenile fish? Water Air Soil Pollut. 228 (12), 470 https://doi.org/10.1007/s11270-017-3654-4.

Nortvedt, R., Tuene, S., 1998. Body composition and sensory assessment of three weight groups of Atlantic halibut (Hippoglossus hippoglossus) fed three pellet sizes and three dietary fat levels. Aquaculture 161 (1–4), 295–313. https://doi.org/10.1016/S0044-8486(97)00277-9.

Pata, V., Ahmed, F., Discher, D.E., Dan, N., 2004. Membrane solubilization by detergent: resistance conferred by thickness. Langmuir 20 (10), 3888–3893. https://doi.org/10.1021/la035734e.

Pfeiffer, F., Fischer, E.K., 2020. Various digestion protocols within microplastic sample processing-evaluating the resistance of different synthetic polymers and the efficiency of biogenic organic matter destruction. Front. Environ. Sci. 8, 572424 https://doi.org/10.3389/fenvs.2020.572424.

Phuong, N.N., Zalouk-Vergnoux, A., Kamari, A., Mouneyrac, C., Amiard, F., Poirier, L., Lagarde, F., 2018. Quantification and characterization of microplastics in blue mussels (Mytilus edulis): protocol setup and preliminary data on the contamination of the French Atlantic coast. Environ. Sci. Pollut. Res. 25 (7), 6135–6144. https://doi.org/10.1007/s11356-017-8862-3.

Primpke, S., Wirth, M., Lorenz, C., Gerdts, G., 2018. Reference database design for the automated analysis of microplastic samples based on Fourier transform infrared (FTIR) spectroscopy. Anal. Bioanal. Chem. 410 (21), 5131–5141. https://doi.org/10.1007/s00216-018-1156-x.

Primpke, S., Booth, A.M., Gerdts, G., Gomiero, A., Koegel, T., Lusher, A., Strand, J., Scholz-Boettcher, B.M., Galgani, F., Provencher, J., Aliani, S., Patankarl, S., Vorkamp, K., 2022. Monitoring of microplastic pollution in the Arctic: recent developments in polymer identification, quality assurance and control, and data reporting. Arctic Sci. https://doi.org/10.1139/as-2022-0006.

Richardson, N.E., Meakin, B.J., 1974. Sorption of benzocaine from aqueous-solution by nylon 6 powder. J. Pharm. Pharmacol. 26 (3), 166–174. https://doi.org/10.1111/j.2042-7158.1974.tb09249.x.

Rotjan, R.D., Sharp, K.H., Gauthier, A.E., Yelton, R., Baron Lopez, E.M., CRotjan, R.D., Sharp, K.H., Gauthier, A.E., Yelton, R., Baron Lopez, E.M., Carilli, J., Kagan, J.C., Urban-Rich, J., 2019. Patterns, dynamics and consequences of microplastic ingestion by the temperate coral, Astrangia poculata. Proc. R. Soc. B Biol. Sci. 286 (1905), 1–9. https://doi.org/10.1098/rspb.2019.0726.

Sridharan, S., Kumar, M., Saha, M., Kirkham, M.B., Singh, L., Bolan, N.S., 2022. The polymers and their additives in particulate plastics: what makes them hazardous to the fauna? Sci. Total Environ. 824, 153828 https://doi.org/10.1016/j.scitotenv.2022.153828.

Süssmann, J., Krause, T., Martin, D., Walz, E., Greiner, R., Rohn, S., Fischer, E.K., Fritsche, J., 2021. Evaluation and optimisation of sample preparation protocols suitable for the analysis of plastic particles present in seafood. Food Control 125, 107969. https://doi.org/10.1016/j.foodcont.2021.107969.

Tang, K.H.D., 2021. Interactions of microplastics with persistent organic pollutants and the ecotoxicological effects: a review. Trop. Aquat. Soil Pollut. 1 https://doi.org/10.53623/tasp.v1i1.11 (24-23).

Thiele, C.J., Hudson, M.D., Russell, A.E., 2019. Evaluation of existing methods to extract microplastics from bivalve tissue: adapted KOH digestion protocol improves filtration at single-digit pore size. Mar. Pollut. Bull. 142, 384–393. https://doi.org/10.1016/j.marpolbul.2019.03.003.

Thiele, C.J., Hudson, M.D., Russell, A.E., Saluveer, M., Sidaoui-Haddad, G., 2021. Microplastics in fish and fishmeal: an emerging environmental challenge? Sci. Rep. 11 (1), 2045 https://doi.org/10.1038/s41598-021-81499-8.

Tian, Y., Violet Zhang, H., Kiick, K.L., Saven, J.G., Pochan, D.J., 2017. Transition from disordered aggregates to ordered lattices: kinetic control of the assembly of a computationally designed peptide. Org. Biomol. Chem. (29) https://doi.org/10.1039/C7OB01197K.

Toto, B., Refosco, A., Dierkes, J., Kogel, T., 2023. Efficient extraction of small microplastic particles from rat feed and feces for quantification. Heliyon 9 (1), e12811. https://doi.org/10.1016/j.heliyon.2023.e12811.

Van Cauwenberghe, L., Janssen, C.R., 2014. Microplastics in bivalves cultured for human consumption. Environ. Pollut. 193, 65–70. https://doi.org/10.1016/j.envpol.2014.06.010.

Vandermeersch, G., Van Cauwenberghe, L., Janssen, C.R., Marques, A., Granby, K., Fait, G., Kotterman, M.J.J., Diogene, J., Bekaert, K., Robbens, J., Devriese, L., 2015. A critical view on microplastic quantification in aquatic organisms. Environ. Res. 143, 46–55. https://doi.org/10.1016/j.envres.2015.07.016.

Welch, S.A., Taunton, A.E., Banfield, J.F., 2002. Effect of microorganisms and microbial metabolites on apatite dissolution. Geomicrobiol J. 19 (3), 343–367. https://doi.org/10.1080/01490450290098414.

Wesch, C., Bredimus, K., Paulus, M., Klein, R., 2016. Towards the suitable monitoring of ingestion of microplastics by marine biota: a review. Environ. Pollut. 218, 1200–1208. https://doi.org/10.1016/j.envpol.2016.08.076.